Kinetic Conditions for Living and Controlled Free Radical Polymerizations Mediated by Reversible Combination of Transient Propagating and Persistent Radicals: The Ideal Mechanism

Marc Souaille and Hanns Fischer*

Physikalisch-Chemisches Institut der Universität Zürich, Winterthurerstrasse 190, CH 8057 Zürich, Switzerland

Received April 19, 2000; Revised Manuscript Received July 26, 2000

ABSTRACT: A full kinetic analysis is presented for living polymerizations controlled by the reversible combination of growing propagating and persistent radicals. Analytical equations are derived for the concentrations of the radicals, the dormant and unreactive polymer chains, the monomer, the number-average degree of polymerization, and the polydispersity. In the absence of side reactions, these specify optimum ranges of rate constants of the dissociation and combination to ensure, for specific monomers, formation of products with preset molecular weights, predictable small fractions of unreactive polymer, and low polydispersities in predictable conversion times. The theoretical conclusions agree with experimental findings for alkoxyamine initiators. Consideration of borderline cases shows that a living and controlled radical polymerization can degenerate to give living polymers with no apparent control of molecular weight and polydispersity or can produce mainly unreactive polymers with regulated molecular weight and small polydispersity. The chain-length and viscosity dependence of the self-termination constant does not change the overall mechanism but does affect the polymerization rate.

Introduction

Living polymerizations provide polymers that are able to grow whenever additional monomer is supplied.[1] Hence, the chains can be extended later on, and block copolymers can be produced. Today, this is mainly achieved by anionic and cationic processes which, under sufficiently rigorous conditions, suffer little from termination.[2] They also offer initiation periods that are short compared to the overall polymerization time. Hence, all chains start to grow essentially instantaneously. The degree of polymerization increases linearly with monomer conversion and is inversely proportional to the initiator concentration. The width of the chain length distibution grows slower than the degree of polymerization; i.e., the polydispersity index decreases with time, and the polymer retains the reactive ionic or ion pair end groups. Such polymerizations are often also called regulated or controlled.

Conventional free radical polymerizations employ continuous initiation, and the polymers are mostly formed by termination of the growing chain radicals in coupling or disproportionation reactions.[2] This leads to unreactive (dead) polymers with essentially time-invariant degrees of polymerization and broad molecular weight distributions. However, in recent years, the ease and robustness of radical polymerizations have been combined with the advantages of ionic reactions, and the new radical processes also provide living polymers with regulated molecular weights and low polydispersities.[1−8]

One successful scheme involves the reversible combination of growing chain radicals $R_n^\bullet$ (with n monomer units (M)) with persistent radical species $Y^\bullet$ to dormant polymer chains R_n−Y; i.e., the mechanism described by reactions 1−3.

$$R_n\text{−Y} \xrightarrow{k_d} R_n^\bullet + Y^\bullet \quad (1)$$

$$R_n^\bullet + Y^\bullet \xrightarrow{k_c} R_n\text{−Y} \quad (2)$$

$$R_n^\bullet + M \xrightarrow{k_p} R_{n+1}^\bullet \quad (3)$$

The products of the irreversible terminations, such as

$$R_n^\bullet + R_m^\bullet \xrightarrow{k_t} P_n + P_m \quad (4)$$

are virtually absent. The concentration of the transient growing radicals $R_n^\bullet$ are low, and there is a remarkably large excess of the persistent species $Y^\bullet$. Rizzardo et al.[3] introduced alkoxyamines R_0−Y as initiators where R_0 is an alkyl and Y is a nitroxide group. Later, Georges et al.[4] found that the polymerization can also be started with a conventional radical initiator in the presence of a stable nitroxide $Y^\bullet$. In this case, the alkoxyamines R_n−Y are formed in situ. Today, many variants are known which use different initiators, different persistent radicals, and different procedures.[5]

In general terms, this radical polymerization resembles the so-called iniferter technique of Otsu[6] where the persistent radical itself initiates and the remainder of the mechanism is as given by reactions 1−3. Furthermore, it is intrinsically related to the atom transfer radical polymerization (ATRP) of Otsu, Matyjaszewski, Percec, and Sawamoto.[6,7] In this system, the dormant chains are capped by halogen atoms which are reversibly transferred to metal complexes in the lower oxidation state. This generates the transient growing radicals

* Corresponding author. Fax: 0041 1 635 68 56. E-mail: hfischer@pci.unizh.ch.

10.1021/ma000689s CCC: $19.00
Published on Web 09/15/2000

and complexes in the higher oxidation state, and the latter ($Me^{(k+1)+}Hal$) are the persistent species.

$$R_n{-}Hal + Me^{k+} \xrightarrow{k_{act}} R_n^{\bullet} + Me^{(k+1)+}Hal \qquad (5)$$

$$R_n^{\bullet} + Me^{(k+1)+}Hal \xrightarrow{k_{deact}} R_n{-}Hal + Me^{k+} \qquad (6)$$

There are also similarities to the reversible addition fragmentation transfer scheme (RAFT) which is based on an exchange reaction[8]

$$R_n^{\bullet} + R_m{-}X \xrightarrow{k_{ex}} R_n{-}X + R_m^{\bullet} \qquad (7)$$

in addition to initiation and propagation steps.

In all radical polymerizations, the active species are carbon-centered free radicals. These transient species always disappear by self-termination (eq 4) which is at least close to diffusion control. Therefore, the questions arise why only minor amounts of dead polymer chains are obtained in processes such as (1−4) and what causes the large excess of the persistent over the transient radicals. For the mechanism in (1−4) and for ATRP the reason is the operation of the persistent radical effect,[9] which is known in other parts of chemistry.[10] This effect is easily explained. Consider the reversible dissociation, e.g., of an alkoxyamine, in the absence of monomer or other radical scavenging agents into a transient and a persistent radical. The reactions are

$$R{-}Y \xrightarrow{k_d} R^{\bullet} + Y^{\bullet} \qquad (8)$$

$$R^{\bullet} + Y^{\bullet} \xrightarrow{k_c} R{-}Y \qquad (9)$$

$$R^{\bullet} + R^{\bullet} \xrightarrow{k_t} 2P \qquad (10)$$

If one starts only with R−Y, the radicals $R^{\bullet}$ and $Y^{\bullet}$ appear initially in equal concentrations because they are formed with equal rate. When their concentrations become large enough, the bimolecular processes (9) and (10) set in. Self-termination (10) removes $R^{\bullet}$ irreversibly, but the group Y stays in the pool of R−Y and free $Y^{\bullet}$. Hence, the self-termination of $R^{\bullet}$ causes, by simple stoichiometry, a build-up of excess $Y^{\bullet}$. This process continues as time proceeds, and, hence, the excess of $Y^{\bullet}$ increases, and the cross-coupling (eq 9) becomes more and more favored over the self-termination (eq 10). The lifetime of the radical precursor R−Y is prolonged, often by many orders of magnitude, and there seems to be no net reaction. In polymerizations, $R^{\bullet}$ transforms to $R_n^{\bullet}$, and, in the course of time, R_n−Y, the dormant chains, become the product which dominates over the dead polymers formed by the self-termination of $R_n^{\bullet}$.

This purely kinetic effect reproduces the observed selectivity of dormant polymer formation and the features of control for the basic mechanism (eqs 1−4) quite well.[9] There is an intermediate quasi-equilibrium stage of the reversible bond dissociation (eqs 1 and 2) with weakly time-dependent radical concentrations and a large excess of $Y^{\bullet}$. Furthermore, we have derived approximate analytic equations for the polymerization rate, the degree of polymerization, and the polydispersity which agree with observations. Also, we found some necessary conditions for the rate constants of the basic reactions which are required for a successful process.

Actually, there must be quite stringent kinetic criteria for the existence of the persistent radical effect itself and for its operation during living radical polymerization. First, an extended quasi-equilibrium stage with a small concentration of $R^{\bullet}$ and a large excess of $Y^{\bullet}$ can exist only for a limited period since for infinite time, the never ceasing, though always decelerating, self-termination must ultimately lead to complete conversion of the R groups to dead products. To obtain living polymers, monomer conversion must occur in the quasi-equilibrium stage, and must be complete before the end of this period. Moreover, the quasi-equilibrium cannot be established if the rate constant of the cross-reactions 2 or 6 are small. Second, the rate constant of radical formation by reactions 1 or 5 must be large to ensure a quasi-instant start of the process in comparison to the overall monomer conversion time. If this is not the case, the polydispersities should be large as in a conventional polymerization even though the polymer may still be living. Third, the optimum rate constants of bond dissociation and reformation must depend on the propagation rate constant of the monomer, since a too fast propagation will also deteriorate the control.

To extend the insight into the underlying kinetics, we have now reanalyzed the kinetic scheme for the ideal reaction mechanism of living polymerizations regulated by persistent radicals (eqs 1−4) to a greater detail and in a mathematically much more elegant and rigorous way. This enables us to state more precise conditions for the relevant rate constants. These ensure the formation of polymers with predictable low contents of dead species, predictable degrees of polymerization, predictable low polydispersities and in preset polymerization times. We also found some new features of the process. For borderline rate constants, polymers are predicted that are living but not controlled or are controlled without being living.

In the following, we first reexplore the kinetics of reactions 8−10; i.e., the persistent radical effect in the absence of monomer. The results are then coupled to the propagation reaction. The major emphasis will be on the analytical treatment which is supported by numerical calculations.

For polymerization systems we restrict the analysis to the minimum reactions 1−4 with only disproportionation as irreversible termination since this facilitates the treatment of the moments. Irreversible termination by combination does not change the features of the process, since it simply doubles the degree of polymerization of the unreactive polymer fraction. We also use chain-length independent rate constants but comment on the effects of a varying termination constant k_t. Extensions of the analysis to experimental conditions that use an initial excess of the persistent radical to improve control, use extra conventional initiation or the destruction of $Y^{\bullet}$ to shorten conversion times, allow for combination and for side reactions as the disproportionation of the transient and the persistent radical, and cover ATRP and the iniferter technique will be published in due course.

Before presenting the calculations, we must stress that they refer to the ideal case. In practice, there are many important side reactions that may blur the kinetics but the main characteristics should remain intact.

The Persistent Radical Effect

Kinetic Equations and Previous Solutions. In this section, we consider only reactions 8−10 and abbreviate R−Y as I, R• as R, and Y• as Y. The initial conditions for the concentrations are

$$[\mathrm{R{-}Y}](t=0) = [\mathrm{I}](t=0) = [\mathrm{I}]_0 \neq 0$$
$$[\mathrm{Y}]_0 = [\mathrm{R}]_0 = [\mathrm{P}]_0 = 0 \quad (11)$$

By stoichiometry and for termination by disproportionation only, one has the relations between the concentrations as

$$[\mathrm{I}]_0 - [\mathrm{I}] = [\mathrm{Y}] = [\mathrm{R}] + [\mathrm{P}] \quad (12)$$

This suggests that we should select [R] and [Y] as the only relevant time-dependent variables. The kinetic equations for [R] and [Y] read for homogeneous reaction conditions[11]

$$\frac{\mathrm{d}[\mathrm{R}]}{\mathrm{d}t} = k_\mathrm{d}([\mathrm{I}]_0 - [\mathrm{Y}]) - k_\mathrm{c}[\mathrm{R}][\mathrm{Y}] - k_\mathrm{t}[\mathrm{R}]^2 \quad (13)$$

$$\frac{\mathrm{d}[\mathrm{Y}]}{\mathrm{d}t} = k_\mathrm{d}([\mathrm{I}]_0 - [\mathrm{Y}]) - k_\mathrm{c}[\mathrm{R}][\mathrm{Y}] \quad (14)$$

Because of physical reasons, all rate constants and concentrations are positive or zero. The kinetic equations depend on four parameters, namely k_t, k_d, k_c, and $[\mathrm{I}]_0$. As before,[9] we find it convenient to use a set of reduced parameters that underline the kinetically relevant ratios

$$a = \frac{k_\mathrm{c}[\mathrm{I}]_0}{k_\mathrm{d}} \quad b = \frac{k_\mathrm{t}[\mathrm{I}]_0}{k_\mathrm{d}} \quad (15)$$

use reduced concentrations and time

$$\rho = \frac{[\mathrm{R}]}{[\mathrm{I}]_0} \quad \eta = \frac{[\mathrm{Y}]}{[\mathrm{I}]_0} \quad \tau = k_\mathrm{d}t \quad (16)$$

and define $\dot{x} = \mathrm{d}x/\mathrm{d}\tau$. In terms of these parameters, (13) and (14) are

$$\dot{\rho} = 1 - \eta - a\rho\eta - b\rho^2 \quad (17)$$

$$\dot{\eta} = 1 - \eta - a\rho\eta \quad (18)$$

with the initial conditions $\rho(\tau=0) = \eta(\tau=0) = 0$. From (17) and (18) the kinetics of the reduced concentrations are completely determined by the parameters a and b. It is thus sufficient to solve the nonlinear differential equations in terms of a and b and then go back to the real concentrations and times by using the scaling relations 15 and 16.

Parameters a and b are determined by the values of $[\mathrm{I}]_0$ and the rate constants, and reasonable values can be taken from the literature. In polymerizations, one often aims at average degrees of polymerization of 100−1000 for an initial monomer concentration of about 10 M (bulk). Hence, $[\mathrm{I}]_0 = 10^{-2}$ to 10^{-1} M. For small radicals R• and low viscosity media, the termination constant is usually $k_\mathrm{t} \cong 10^9$ $\mathrm{M^{-1}s^{-1}}$,[12] and it reduces to averages of 10^7 to 10^8 $\mathrm{M^{-1}s^{-1}}$ for polymeric radicals depending on chain length and to even lower values at high conversions.[13] For the special case of alkoxyamines, the cross-coupling rate constants are in the range $k_\mathrm{c} = 10^8$ to 10^9 $\mathrm{M^{-1}\,s^{-1}}$ for small alkyl and nitroxide species[14] and may become as low as 10^5 to 10^6 $\mathrm{M^{-1}\,s^{-1}}$ because of steric hindrance.[15] Finally, k_d has been measured for simple[16,17] and polymeric[18] alkoxyamines and ranges from 10^{-6} to 1 $\mathrm{s^{-1}}$ for typical reaction temperatures around 120 °C. This places the parameters a between 10^3 and 10^{14} and b between 10^5 and 10^{14}. Both a and b are always large compared to 1, and $a^2/b \gg 1$ for many cases.

Earlier,[9] we converted eqs 17 and 18 into nonlinear second-order differential equations for each variable ρ and η separately, and found approximate solutions via a power law Ansatz, e.g., $\eta = \beta\tau^\alpha$. The second-order differential equations were fulfilled for specific parameters α and β, and this revealed that the time evolution of the concentrations exhibits three distinct stages.

Initially, the concentrations of both radicals increase linearly with time, i.e.

$$\eta = \rho = \tau \quad \text{or} \quad [\mathrm{Y}] = [\mathrm{R}] = k_\mathrm{d}[\mathrm{I}]_0 t \quad (19)$$

This is followed by a stage where the radical concentrations depend on the third root of time

$$\eta = \left(\frac{3b}{a^2}\right)^{1/3}\tau^{1/3} \quad \rho = \left(\frac{1}{3ab}\right)^{1/3}\tau^{-1/3} \quad \text{or}$$
$$[\mathrm{Y}] = (3k_\mathrm{t}K^2[\mathrm{I}]_0{}^2)^{1/3}t^{1/3} \quad [\mathrm{R}] = (K[\mathrm{I}]_0/3k_\mathrm{t})^{1/3}t^{-1/3} \quad (20)$$

where $K = k_\mathrm{d}/k_\mathrm{c}$ is the equilibrium constant of the reversible dissociation of R−Y, and there is an equilibrium relation

$$a\rho\eta = 1 \quad \text{or} \quad k_\mathrm{c}[\mathrm{R}][\mathrm{Y}] = k_\mathrm{d}[\mathrm{I}]_0 \quad (21)$$

This relation differs from the normal law of mass action because it contains the initial concentration $[\mathrm{I}]_0$ instead of the momentary value [I]. Also, the radical concentrations in (21) are time dependent though this time dependence cancels out to produce a time-independent expression. Therefore, we call this stage a *quasi-equilibrium*. The process ends with a period in which [Y] has nearly attained its final value $[\mathrm{I}]_0$, and [R] decreases inversely proportional to t.

The kinetic condition for the existence of the quasi-equilibrium was previously obtained from the time boundaries of the different stages as

$$a^2/b > 4 \quad \text{or} \quad \mathrm{K}/[\mathrm{I}]_0 < k_\mathrm{c}/4k_\mathrm{t} \quad (22)$$

If it is not fulfilled, the initial stage proceeds directly to the final stage without the intermediate quasi-equilibrium. The experimental data given above indicates that $a^2/b \gg 1$ often holds for the reversible dissociation of alkoxyamines, and therefore, the quasi-equilibrium situation should exist. This has been demonstrated experimentally.[9,19]

Now, eqs 17 and 18 are analyzed in a different more rigorous way. The principle features of the former solutions remain valid, but there are additional subtleties.

Phase Diagram Analysis. In the analysis of systems of two nonlinear differential equations such as (17) and (18) for the dynamical variables ρ and η, one often starts with a discussion of the trajectories of the point $(\rho(\tau),\eta(\tau))$ in the two-dimensional phase plane spanned by the possible values of the variables ρ and η.[20] Since ρ, η, a, and b are positive or zero, the limits of the phase space

available to ρ and η are easily derived. If one sets $a = b = 0$ in eqs 17 and 18 and the initial condition $\rho(\tau = 0) = \eta(\tau = 0) = 0$ is obeyed, one obtains the solution

$$\tilde{\rho} = \tilde{\eta} = 1 - e^{-\tau}$$

For positive a and b, eqs 17 and 18 require that $\rho \leq \tilde{\rho}$ and $\eta \leq \tilde{\eta}$ for all times ($\forall t$); i.e., as $\tilde{\rho}$ and $\tilde{\eta}$, the variables ρ and η are restricted to values between 0 and 1. Moreover, from (17) and (18) one has

$$\dot{\eta} = \dot{\rho} + b\rho^2 \tag{23}$$

and with the initial condition this implies that $\eta \geq \rho \forall t$. Hence, all trajectories are in the plane $(0,1) \times (0,1)$, are positioned along or over the first diagonal, and start at the origin (0,0). Setting $\dot{\eta} = 0$ and $\dot{\rho} = 0$, eqs 17 and 18 lead to the singular point (0,1), which is stable. This confirms that, at infinite time, [Y] and [R] reach the final values $[Y]_\infty = [I]_0$ and $[R]_\infty = 0$.

The shape of the trajectories follows from an identification of the isoclines where the time derivatives of the individual dynamic variables are zero.

Isocline $\eta_1(\rho)$ Where $\dot{\eta} = 0$. From (18), one has eq 24.

$$\eta_1(\rho) = \frac{1}{1 + a\rho} \tag{24}$$

If $\eta < \eta_1$, then $\dot{\eta} > 0$, i.e., η increases with time, and if $\eta > \eta_1$, then $\dot{\eta} < 0$, i.e., η decreases. For $\eta = \eta_1$, $d\eta/d\rho = 0$, and $\dot{\rho} = -b\rho^2$ is negative. Consequently, any trajectory can cross the isocline η_1 only horizontally and in the direction of decreasing ρ.

Isocline $\eta_2(\rho)$ Where $\dot{\rho} = 0$. From (17), one has eq 25.

$$\eta_2(\rho) = \frac{1 - b\rho^2}{1 + a\rho} \tag{25}$$

If $\eta < \eta_2$, then $\dot{\rho} > 0$, and if $\eta > \eta_2$, then $\dot{\rho} < 0$. For $\eta = \eta_2$, $d\eta/d\rho = \infty$ and $\dot{\eta} = +b\rho^2$. Consequently, any trajectory can cross the isocline η_2 only vertically in the direction of increasing η. Further, we note that η_2 crosses the line $\eta = 0$ at the maximum $\rho = 1/\sqrt{b}$. Both isoclines coincide in the singular point (0,1) and approach it with the same slope $d\eta/d\rho = -a$.

Figure 1 shows a computed trajectory in a linear representation for small parameters a and b. Starting from the origin (0,0), both ρ and η increase at first along the first diagonal. Then the trajectory bends up and crosses the isocline η_2 ($\dot{\rho} = 0$) vertically. After this crossing, ρ decreases and η continues to increase. The trajectory cannot cross η_2 a second time since it must do so vertically in the direction of increasing η. It cannot cross the isocline η_1 ($\dot{\eta} = 0$) either since it must do so horizontally in the direction of decreasing ρ. Therefore, after the first crossing, the trajectory is confined to the region between the two isoclines. This also means that it approaches the final point (0,1) with the same slope as the two isoclines, namely $d\eta/d\rho = -a$. The maximum of ρ is on isocline η_2. There, ρ is limited to values below $\rho = 1/\sqrt{b}$, and hence, one has $\rho \leq 1/\sqrt{b}\ \forall t$.

As mentioned before, in real systems we expect large parameters $a \gg 1$ and $b \gg 1$ and $a^2/b \gg 1$. The latter ratio determines the existence of the persistent radical effect. Figure 2 shows computed trajectories and the isoclines for four different sets of the parameters (a,b)

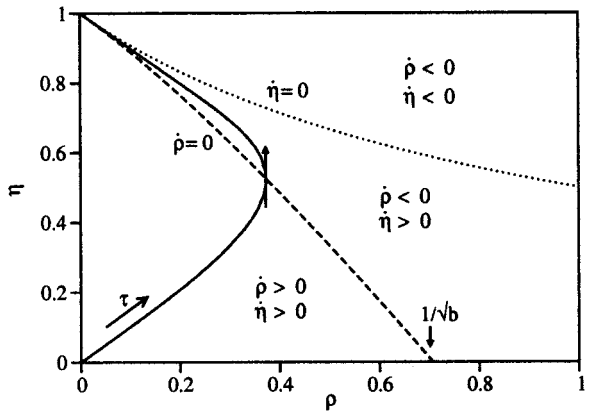

Figure 1. Example of a trajectory of the point (ρ,η); i.e., the reduced concentrations of the radicals R• and Y•, and the isoclines $\dot{\rho} = 0$ (dashed) and $\dot{\eta} = 0$ (dotted) in the phase plane. For the sake of clarity, small values of the parameters $a = 1$ and $b = 2$ have been chosen.

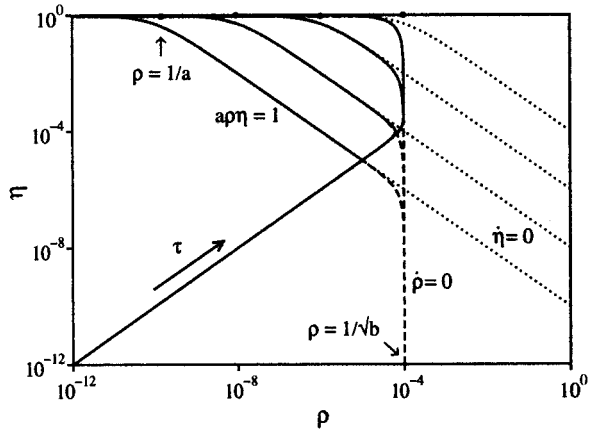

Figure 2. Trajectories of the point (ρ,η); i.e., the reduced concentrations of the radicals R• and Y•, and the isoclines $\dot{\rho} = 0$ (dashed) and $\dot{\eta} = 0$ (dotted) in the phase plane. Sets of parameters from left to right and from down to up $(a,b) = (10^{10},10^8)$, $(10^8,10^8)$, $(10^6,10^8)$, and $(10^4,10^8)$.

corresponding to $a^2/b = 10^{12}$, 10^8, 10^4, and 1 in a log−log representation. The parameter b is kept constant at $b = 10^8$, i.e., it is in the center of the possible range.

Since the trajectories are strongly linked to the isoclines we discuss first the dependence of the isoclines on the parameters a and b and start from the singular point. As easily derived from eqs 24 and 25, both isoclines leave the singular point horizontally because $d(\log \eta)/d(\log \rho) = \rho/\eta \times d\eta/d\rho = 0$ at the singular point. They follow the line $\eta = 1$ as long as $\rho \ll 1/a$ and $\rho \ll 1/\sqrt{b}$. After ρ reaches $\rho \cong 1/a$ (marked points), the isocline η_1 ($\dot{\eta} = 0$) becomes close to the function $\eta = 1/a\rho$ or $a\rho\eta = 1$, which is a diagonal with negative slope in the double logarithmic representation. The isocline η_2 behaves as η_1 until $\rho \cong 1/\sqrt{b}$, which is larger than $1/a$ for our set of parameters, and until $\eta \cong \sqrt{b}/a$. Thereafter, it follows the vertical line $\rho = 1/\sqrt{b}$. For the first three cases where $a^2/b \gg 1$, both isoclines closely follow the function $a\rho\eta = 1$ over an extended region, whereas in the last case, with $a^2/b = 1$, there is no such coincidence.

In time, the trajectories start from the origin (0,0), first follow the first diagonal ($\rho = \eta$), then cross η_2 (Figure 1), and finally remain confined between the two isoclines. For all parameters they remain close to $\dot{\rho} = 0$

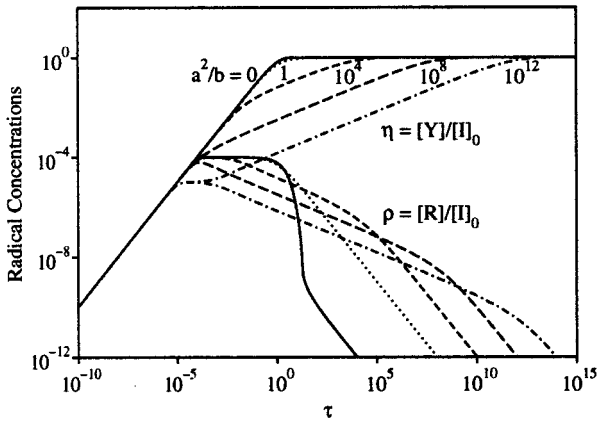

Figure 3. Reduced concentrations of the radicals R• and Y• as functions of the reduced time. Parameters as in Figure 2, $(a,b) = (10^{10},10^8)$, $(10^8,10^8)$, $(10^6,10^8)$, and $(10^4,10^8)$.

after the crossing because then $\dot{\rho} < 0$ is negative and because this isocline cannot be recrossed. In the first two cases of parameters, the crossing occurs in the region where η_1 nearly coincides with $a\rho\eta = 1$, and in the third the trajectory reaches $a\rho\eta = 1$ at higher η. However, in the last case, η_1 and the trajectory do not approach this function, $a\rho\eta = 1$, which is the quasi-equilibrium relation (eq 21). Hence, an intermediate quasi-equilibrium regime exists for the first three sets of parameters of Figure 2 but not for the last one.

The behavior of the trajectories in the phase plane leads the way to derive the necessary and sufficient conditions for the existence of the quasi-equilibrium regime on the trajectory. This is done in the Appendix and gives

$$a^2/b \gg 1 \quad \text{i.e., } K/[I]_0 \ll k_c/k_t \tag{26}$$

and

$$a \gg 1 \quad \text{i.e., } K/[I]_0 \ll 1 \tag{27}$$

Furthermore, we have seen above that ρ is restricted to values between 0 and 1, and that it must obey $\rho \leq 1/\sqrt{b}$ $\forall t$. Therefore, one also has

$$b \geq 1 \quad \text{i.e., } k_d \leq k_t[I]_0 \tag{28}$$

These conditions are sharper than that found previously (eq 22), and conditions 26 and 28 imply condition 27.

Figure 3 displays the time dependencies of the reduced radical concentrations in a log−log plot for the same set of parameters (a,b) as used for Figure 2. For all cases the concentrations of both radicals first increase linearly in time as $\rho = \eta = \tau$ or $[R] = [Y] = k_d[I]_0t$. This also follows directly from the rate equations for small concentrations and corresponds to the first linear part of the trajectories. Then there is a transition region which will be dealt with later on.

For large values of a^2/b, the transition region is followed by a decrease of ρ and an increase of η which appear linear in the log−log plot and have opposite slopes smaller than 1. This regime corresponds to the quasi-equilibrium with $a\rho\eta = 1$, and therefrom $\dot{\rho} = -\dot{\eta}\rho/\eta$. In fact, using these relations in conjunction with eq 23 and rearranging terms gives (29).

$$\dot{\eta}(a\eta^2 + 1) = b/a \tag{29}$$

By integration we get

$$\frac{a}{3}\eta^3 + \eta = \frac{b}{a}(\tau - \tau_0) + C \tag{30}$$

where τ_0 and $C = a/3\eta_0^3 + \eta_0$ are integration constants. Since $\eta > \eta_0$ and $\tau > \tau_0$, the first terms of both sides will dominate for long times; i.e., we reobtain the result of the earlier derivation[9]

$$\eta = \left(\frac{3b}{a^2}\right)^{1/3} \tau^{1/3} \quad \text{or} \quad [Y] = (3k_tK^2[I]_0^2)^{1/3}t^{1/3}$$

and with $a\rho\eta = 1$

$$\rho = \left(\frac{1}{3ab}\right)^{1/3} \tau^{-1/3} \quad \text{or} \quad [R] = (K[I]_0/3k_t)^{1/3}\, t^{-1/3} \tag{20}$$

This derivation of eq 20 resembles that presented by Fukuda et al.,[21] who, however, preassumed the existence of the quasi-equilibrium without further proof and ignored the linear term of the LHS of eq 30. The solutions in (20) must break down when η approaches 1, i.e., at a time given approximately by $\tau = a^2/3b$.

At the end, η follows the line $\eta = 1$ as the trajectories in Figure 2. In this stage, the concentration ρ of the transient species decreases proportional to τ^{-1} (Figure 3). An approximate analytic expression for this regime is obtained from the slope of the trajectory in the singular point (0,1) which is $-a$ (see above). From (17) and (18), one has close to this point

$$\frac{d\eta}{d\rho} = \frac{\dot{\eta}}{\dot{\eta} - b\rho^2} = -a \tag{31}$$

Inserting (23) and rearranging terms, we get

$$\dot{\rho} = -\frac{b}{1+a}\rho^2 \tag{32}$$

which integrates to

$$\rho = \frac{\rho_0}{1 + \rho_0\dfrac{b}{1+a}\tau} \tag{33}$$

and gives at long times

$$\rho = \frac{1+a}{b}\frac{1}{\tau} \tag{34}$$

corresponding to the behavior seen in Figure 3. In our earlier work[9] the long time regime was erroneously described by $\rho = b/\tau$.

To conclude the description of the time dependencies, we now consider the transition from the initial to the intermediate time regime.

(i) For $a \gg b$ in Figure 2, the line $\eta = \rho$ crosses the isocline η_2 ($\dot{\rho} = 0$) in the region where $a\eta\rho = 1$. At the crossing, $\eta \approx \rho \approx 1/\sqrt{a}$, and immediately after the crossing, the time dependence of η is given by the second term of the LHS of eq 30

$$\eta = \frac{b}{a}(\tau - \tau_0) + \eta_0 \tag{35}$$

where $\eta_0 = \tau_0 = 1/\sqrt{a}$ and $\rho = 1/a\eta$. Since $b \ll a$, the second term on the RHS of eq 35 dominates. This means that η (and ρ) remain constant after the crossing at $\eta =$

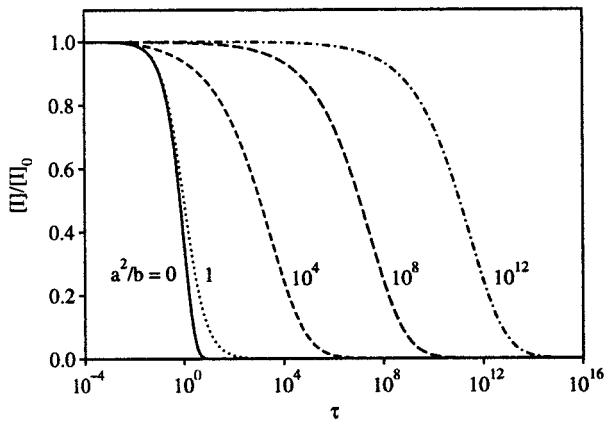

Figure 4. Reduced concentrations of the radical precursor as a function of the reduced time. Parameters as in Figure 2, $(a,b) = (10^{10},10^8)$, $(10^8,10^8)$, $(10^6,10^8)$, and $(10^4,10^8)$.

$\rho = 1/\sqrt{a}$, and comparison with eq 20 shows that this holds for a time of the approximate duration $\sqrt{a}/3b$. In Figure 3, this behavior is exemplified by the case $a^2/b = 10^{12}$.

(ii) For smaller a as $a = b = 10^8$, the portion of the isocline η_1 where $a\rho\eta = 1$ is located at larger values of ρ, and the extent of overlap of η_1 and η_2, i.e., the quasi-equilibrium regime, is reduced. Now, the quasi-equilibrium is entered without an intermediate interval of constant radical concentrations (Figure 3, case $a^2/b = 10^8$).

(iii) For $a \ll b$ but still $a^2/b \gg 1$, the trajectory crosses η_2 in its vertical part where $\rho = 1/\sqrt{b}$. Then ρ stays constant at $\rho = 1/\sqrt{b}$ on η_2, and η increases linearly with time as before the crossing; i.e., $\eta = \tau$. This follows from eq 23 with $\dot{\rho} = 0$ and $\rho = 1/\sqrt{b}$ and holds for a time of approximately $\tau = \sqrt{b}/3a$. Then, the quasi-equilibrium regime is reached (Figure 3, case $a^2/b = 10^4$).

(iv) If a is further decreased such as to $a^2/b = 1$, the isocline η_2 does not contain a region where $a\eta\rho = 1$; i.e., there is no quasi-equilibrium. Now ρ stays constant at $\rho = 1/\sqrt{b}$, and η increases linearly with time until the long time solution (eq 34) is approached.

With decreasing a, the isocline η_1 shifts to the right in the phase plane (Figure 2). Therefore, for sufficiently small a, the behavior of η becomes independent of this parameter. This means that Y• and the precursor R−Y behave as if there were no cross-coupling reaction 9 though the rate constant k_c can be far from zero. This point is emphasized by Figure 4 where the relative concentration of I = R−Y is shown as a function of time for the same sets of parameters as used in Figures 2 and 3. In comparison to the absence of the cross-coupling reaction ($a^2/b = 0$), there is practically no lifetime prolongation of the precursor until $a^2/b = 1$.

For $a^2/b \gg 1$, the lifetime prolongation scales as a^2/b. This is due to the fact that with increasing $a^2/b \gg 1$, the quasi-equilibrium regime becomes more and more extended. Then, the stoichiometry relation $[I]_0 - [I] = [Y]$ and eq 20 yield

$$\frac{[I]}{[I]_0} = 1 - \left(\frac{3b}{a^2}\tau\right)^{1/3} \tag{36}$$

which explains the scaling behavior.

In conclusion, for the ideal reaction scheme (eqs 8−10), the persistent radical effect is characterized by a marked lifetime prolongation of the precursor molecule R−Y, a quasi-equilibrium for the reactions 8 and 9 with a large excess of the persistent over the transient radical and weak time dependencies of the concentrations. During its operation, the yield of the final product P remains small. The effect requires rate constants that fulfill the conditions

$$K/[I]_0 \ll k_c/k_t \quad \text{or} \quad \frac{k_c^{\,2}}{k_d} \gg \frac{k_t}{[I]_0} \tag{26}$$

$$K/[I]_0 \ll 1 \quad \text{or} \quad k_d \ll k_c[I]_0 \tag{27}$$

and

$$k_d \le k_t[I]_0 \tag{28}$$

If condition 26 is not fulfilled, reactions 8−10 take the course of a normal radical process without cross-coupling (eq 9) although k_c can be far from zero.

Living and Controlled Free Radical Polymerization

Conditions for Living Polymer Formation. In the presence of monomer, the transient radicals R• transform to chain growth radicals R_n• by monomer addition (eq 3), and the products R_n-Y of the cross-coupling (eq 2) are the desired dormant chains. Their lifetimes should be larger than the time needed for monomer conversion; i.e., the conversion should occur in the period of the quasi-equilibrium where there is lifetime prolongation. In the following, we take all rate constants of reactions 1−4 as independent of the chain length n, as before,[9] and comment on deviations therefrom in a later section. This simplifies the analytic treatment because one needs to consider only the sums of the concentrations

$$[I] = \sum_0^\infty [I_n] = \sum_0^\infty [R_n{-}Y] \qquad [R] = \sum_0^\infty [R_n] \qquad [P] = \sum_0^\infty [P_n] \tag{37}$$

and has the same initial conditions (eq 11), stoichiometry relations (eq 12) and kinetic equations (eqs 13 and 14) as in the absence of monomer. The only additional equation

$$\frac{d[M]}{dt} = -k_p[R][M] \tag{38}$$

involves the conversion of the monomer M and does not influence the evolution of the concentrations of R• and Y•. Thus, from a formal point of view, the formation of living polymers is described by the coupling of the solution of eq 38 to the solutions (eq 20) for the radical concentrations in the quasi-equilibrium regime.

However, there should be only very little monomer conversion before the onset of this regime. To calculate this fraction we use the reduced quantities

$$\mu = \frac{[M]}{[I]_0} \quad \text{and} \quad c = \frac{k_p[I]_0}{k_d} \tag{39}$$

so that eq 38 becomes

$$\frac{d\mu}{d\tau} - c\rho\mu \tag{40}$$

As has been derived in the earlier section and as seen in Figure 3, ρ increases linearly with time, $\rho = \tau$ before a time τ_1, and for $a \gg b$ and $a \ll b$, ρ then remains constant until time τ_2 at which the quasi-equilibrium is attained. The integration of eq 40 between 0 and τ_2 gives eq 41.

$$\mu(\tau_2) = \mu(0)e^{-c\tau_1(\tau_2 - \tau_1/2)} \tag{41}$$

If $c\tau_1(\tau_2 - \tau_1/2) \ll 1$, there is little conversion in the initial phase.

Now, for $a \gg b$, $\tau_1 = 1/\sqrt{a}$ and $\tau_2 = \sqrt{a}/3b$, and hence, $c\tau_1(\tau_2 - \tau_1/2) = c/3b(1-3b/2a) \approx c/3b = k_p/3k_t$. Therefore, there is negligible conversion in the initial period if

$$\frac{k_p}{3k_t} \ll 1 \tag{42}$$

For $a \ll b$, one has $\tau_1 = 1/\sqrt{b}$ and $\tau_2 = \sqrt{b}/3a$, and, hence, $c\tau_1(\tau_2 - \tau_1/2) = c/3a(1-3a/2b) \approx c/3a = k_p/3k_c$. Little conversion in the initial period now requires that

$$\frac{k_p}{3k_c} \ll 1 \tag{43}$$

For completenes we also mention that in the special case $a = b$, i.e., $k_c = k_t$, the condition becomes $k_p/4k_t \ll 1$. Experimental high values of k_p do not exceed 10^5 M^{-1} s^{-1},[2] and k_t and k_c are normally much larger (see above). Therefore, in practical cases the newly found conditions 42 and 43 are fulfilled.

Insertion of the quasi-equilibrium expression for [R] (eq 20) into eq 38 gives the time dependence of the monomer concentration as eq 44.

$$[M] = [M]_0 e^{-(3/2)k_p(k_d[I]_0/3k_ck_t)^{1/3}t^{2/3}} \quad \text{or}$$

$$\ln\frac{[M]_0}{[M]} = \frac{3}{2}k_p\left(\frac{k_d[I]_0}{3k_ck_t}\right)^{1/3}t^{2/3} \tag{44}$$

This should be compared with the relation

$$[M] = [M]_0 e^{-k_p(r_I/k_t)^{1/2}t} \quad \text{or} \quad \ln\frac{[M]_0}{[M]} = k_p\left(\frac{r_I}{k_t}\right)^{1/2}t \tag{45}$$

for a conventional radical polymerization with constant initiation rate r_I, and also for an ionic living polymerization, if $(r_I/k_t)^{1/2}$ is replaced by the constant concentration of growing chains. The propagation constant k_p enters both expressions in the same way, and the major difference is the weaker time dependence of (44) which is caused by the nonconstant and permanently decreasing radical concentration [R].

In practice, it may be difficult to distinguish (44) from (45). First, the conversions must be measured precisely because errors may cause a seemingly linear time dependence of $\ln([M]_0/[M])$. Second, side effects, such as varying termination constants and additional reactions may interfere (see below). Figure 5 displays five conversion curves for different initial concentrations of R−Y as obtained from eq 44 and numerical computations. The downward curvature is noticeable, and such curvatures have been observed occasionally.[15,21] Forced fits of the linear time dependence (eq 45) to the curves of Figure 5 in the time region from 2500 to 20 000 s gave slopes which scaled as $[I]_0^{\alpha}$, with an apparent reaction order for the initiator of $\alpha = 0.33 \pm 0.02$, and this agrees with the expectation from eq 44. Such reaction orders have also been detected occasionally,[5,7,15,21] but they were seldom taken seriously.

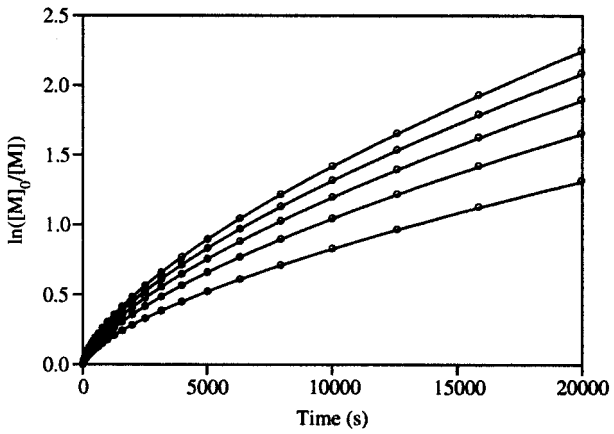

Figure 5. Polymerization index $\ln[M]_0/[M]$ vs time for k_p = 5000 M^{-1} s^{-1}, $k_t = 10^8$ M^{-1} s^{-1}, $k_d = 4.5 \times 10^{-3}$ s^{-1}, $k_c = 2.2 \times 10^7$ $M^{-1}s^{-1}$, $[M]_0 = 10$ M, and $[I]_0 = 0.02$, 0.04, 0.06, 0.08, and 0.1 M by numerical solution and according to eq 44 (circles).

From (44) the time for 90% monomer conversion becomes

$$t_{90} = \frac{(2\ln(10))^{3/2}}{3k_p^{3/2}}\left(\frac{k_t}{K[I]_0}\right)^{1/2} \tag{46}$$

where $K = k_d/k_c$ is the equilibrium constant of the reversible dissociation. The rate constants of dissociation (k_d) and cross-coupling (k_c) do not enter the polymerization time individually, and obviously, short conversion times require large equilibrium constants.

Essentially only living polymer will be formed if t_{90} is smaller than the time required for the formation of a small concentration fraction $\phi = [P]/[I]_0$ of dead products P. From the stoichiometry one has [P] = [Y], and ignoring the formation of P before the quasi-equilibrium, (20) leads to the time required for the formation of a fraction ϕ of [P]

$$t_\phi = \phi^3\frac{[I]_0}{3k_tK^2} \tag{47}$$

Equating (46) and (47) gives the equilibrium constant for which a polymerization to 90% conversion should show a concentration fraction ϕ of dead and a fraction $1 - \phi$ of living polymers

$$K_{90,\phi} = \frac{k_p[I]_0}{2\ln(10)k_t}\phi^2 \tag{48}$$

and reinsertion into (46) provides the corresponding time for 90% conversion

$$t_{90,\phi} = \frac{(2\ln(10))^2k_t}{3k_p^2[I]_0\phi} \tag{49}$$

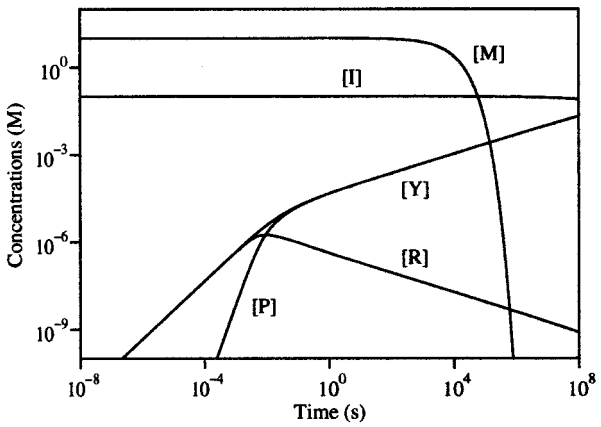

Figure 6. Time evolution of concentrations for a polymerization within the quasi-equilibrium. Parameters: $k_t = 10^8$ M^{-1} s^{-1}, $k_p = 5000$ M^{-1} s^{-1}, $k_c = 2.2 \times 10^7$ M^{-1} s^{-1}, $k_d = 4.5 \times 10^{-3}$ s^{-1}, $[I]_0 = 0.1$ M, and $[M]_0 = 10$ M.

This time does not depend explicitely on the rate constants k_d and k_c though these determine ϕ via K, of course. For example, with $k_p = 2000$ M^{-1} s^{-1}, $k_t = 10^8$ M^{-1} s^{-1}, and $[I]_0 = 0.1$ M, i.e., rate constants for styrene polymerizations at 120 °C,[9] Equation 49 yields a (mimimum) time of 9.81 h for 90% conversion and 5% dead polymer, and the required equilibrium constant is $K_{90,5} = 1.08 \times 10^{-11}$ M. Larger equilibrium constants give shorter times at the expence of larger fractions of unreactive polymer.

To complete this section, Figure 6 shows computed time dependencies of the concentrations of all reaction partners for a living polymerization in one double logarithmic plot. At very short times, the radical concentrations [R] and [Y] increase linearly with time while [P] evolves as t^2. When [R] is sufficiently high for appreciable self-termination, the persistent radical effect sets in. After reaching a maximum, [R] then decreases as $t^{-1/3}$ whereas [Y] increases as $t^{1/3}$. In this regime, [R] is much smaller than [Y], and [P] = [Y]. For the chosen parameters the monomer is fully consumed in the quasi-equilibrium regime. It is nearly completely incorporated into the dormant chains [I] which still have a concentration close to that of the initiating compound $[I]_0$.

Kinetic Conditions for Controlled and Living Radical Polymerizations. Two experimentally accessible quantities which characterize the chain length distribution of polymers are the number-average degree of polymerization

$$X_n = \frac{m_1}{m_0} \tag{50}$$

and the polydispersity index

$$\mathrm{PDI} = \frac{m_0 m_2}{{m_1}^2} \tag{51}$$

defined here in terms of the moments[2]

$$m_k = \sum_{n=1}^{\infty} n^k([I_n] + [P_n] + [R_n]) \quad k = 0, 1, 2$$

The exclusion of $n = 0$ in the summation ensures that only monomer-containing species are counted. If $n = 0$ were included, the zeroth moment would be equal to $[I]_0$ because of the stoichiometry relations (eq 12). Hence, one has

$$m_0 = [I]_0 - ([I_0] + [P_0] + [R_0]) \tag{52}$$

where $[I_0]$, $[P_0]$, and $[R_0]$ are the concentrations of the initiator, the transient radicals and the products which do not contain monomer units. It seems reasonable to assume and is borne out by numerical calculations that I_0 decomposes irreversibly because $R_0^\bullet$ immediately propagates. For the same reason, $[R_0]$ and $[P_0]$ are small compared to $[I_0]$. Thus

$$[I_0] = [I]_0 e^{-k_d t} \tag{53}$$

and

$$m_0 = [I]_0(1 - e^{-k_d t}) \tag{54}$$

For the moments m_1 and m_2 we have the kinetic equations[9]

$$\frac{dm_1}{dt} = -\frac{d[M]}{dt} \tag{55}$$

$$\frac{dm_2}{dt} = -\frac{d[M]}{dt} + 2k_p[M]m_1(R) \tag{56}$$

where $m_1(R) = \sum_{n=1}^{\infty} n[R_n]$. Integrating (55) and using (50) and (54), we obtain the number-average degree of polymerization given in eq 57.

$$X_n = \frac{[M]_0 - [M]}{[I]_0(1 - e^{-k_d t})} \tag{57}$$

For sufficiently long times X_n increases linearly with increasing conversion $[M]_0 - [M]$, and reaches the final value $[M]_0/[I]_0$. This is typical for a controlled process. Deviations from the linear increase at short times are due to the finite time for initiator decomposition. Their observation should allow the determination of k_d. Equation 57 differs from expressions given earlier[9] which did not take the residual initiator concentration properly into account.

The steps involved in the integration of the equation for the second moment m_2 (eq 56) in the quasi-equilibrium regime were explained earlier in some detail[9] and are not repeated here. However, the use of the improved relation for the zeroth moment (eq 54) in (50) leads to a modified equation for the polydispersity index given by (58) where erf is the error function.

$$\mathrm{PDI} = 1 - e^{-k_d t} + \frac{1}{X_n} + \frac{{[M]_0}^2}{([M]_0 - [M])^2}(1 - e^{-k_d t}) \times \left(\frac{\pi {k_p}^3 [I]_0}{k_d k_c k_t}\right)^{1/2} \mathrm{erf}\left[(3k_p)^{1/2}\left(\frac{K[I]_0}{3k_t}\right)^{1/6} t^{1/3}\right] \tag{58}$$

For infinite time, this gives

$$\mathrm{PDI}_\infty = 1 + \frac{[I]_0}{[M]_0} + \left(\frac{\pi {k_p}^3 [I]_0}{k_d k_c k_t}\right)^{1/2} \tag{59}$$

If one sets $e^{-k_d t} = 0$ and omits the last terms of eqs 58 and 59, the expressions for the degree of polymerization

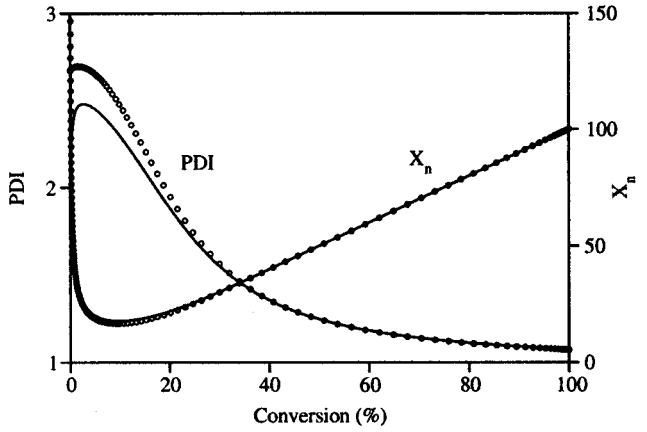

Figure 7. Evolution of the total number-average degree of polymerization X_n and of the total polydispersity index PDI with conversion during a polymerization within the quasi-equilibrium. Parameters: $k_t = 10^8$ M^{-1} s^{-1}, $k_p = 5000$ M^{-1} s^{-1}, $k_c = 2.2 \times 10^7$ M^{-1} s^{-1}, $k_d = 4.5 \times 10^{-3}$ s^{-1}, $[I]_0 = 0.1$ M, and $[M]_0 = 10$ M. Solid lines from numerical calculation; circles from the analytic expressions.

X_n and for the polydispersity index PDI become identical to those holding for a polymerization without termination.[2] Hence, the persistent radical effect with its effective suppression of self-termination leads to a control of the radical polymerization as ionic processes where self-terminations are naturally unlikely, although for a quite different reason.

From eq 59, we define a residual PDI at long times as $\delta = \mathrm{PDI}_\infty - 1 - [I]_0/[M]_0$. This is linked to the rate constants of the reversible bond dissociation by

$$k_d k_c = \frac{\pi k_p{}^3 [I]_0}{k_t} \frac{1}{\delta^2} \tag{60}$$

Obviously, large values of both k_d and k_c favor low final polydispersities, and these are easier to reach for small propagation constants.

Figure 7 shows the dependence of X_n and PDI for the sum of all species I_n, $R_n^\bullet$, and P_n on the momomer conversion as computed by numerical integration of the differential equations of the moments and as obtained from the analytical formulas 57 and 58 for the same parameters as used for Figure 6. For X_n the agreement is excellent while the deviations for PDI at small conversions and early times are due to the approximations made in the derivation of m_2.[9] Both quantities show the effect of the noninstantaneous initiation ($k_d{}^{-1} = 220$ s) at low conversions.

More insight into the course of the polymerization is offered by the time dependence of the chain length distributions given in Figures 8. These were obtained by numerical integrations of the individual coupled kinetic equations for I_n, $R_n^\bullet$, P_n, Y, and M with $n = 0-160$ and $n > 160$ as closure terms and with the same parameters as used for Figures 6 and 7. The distributions for the sum of all species were normalized to equal areas, and the same scaling was also applied to the individual species. It exaggerates the amplitudes at small times, since in reality the total area increases as m_0, but it makes certain features more clearly visible. At very short times, there are (very few) transient radicals R which grow in time to considerable length and form unreactive polymer with a very broad distribution as in a conventional radical polymerization. This process ends after [R] has passed its maximum (Figure 5) and the quasi-equilibrium has developed. Then, there are essentially only dormant chains I, and their rate of formation maximizes approximately at the initiator lifetime $\tau_d = k_d{}^{-1} = 220$ s. After a few lifetimes τ_d, the chain length distribution of I attains a maximum. This shifts continuously to larger chain lengths, and after about 10 h the theoretical limit of 100 is approached.

Optimum Rate Constants for Reversible Dissociation Mediated Living Radical Polymerizations and Borderline Cases. In the following section, we seek criteria for the rate constants k_d and k_c which for a given monomer (k_p), a desired final degree of polymerization ($[I]_0$), and a given self-termination constant lead to a living and controlled free radical polymerization mediated by the reversible bond cleavage.

(i) First, we want the concentration fraction of the dead polymer products $\phi = [P]/[I]_0$ at a large monomer conversion of 90% to be below an allowed upper limit $\hat{\phi}$. From eq 48 this requires

$$K = \frac{k_d}{k_c} \le \frac{k_p [I]_0}{2 \ln(10) k_t} \hat{\phi}^2 \tag{61}$$

(ii) Second, the residual polydispersity index should be smaller than an upper limit $\hat{\delta}$, and, hence, from eq 60

$$k_d k_c \ge \frac{\pi k_p{}^3 [I]_0}{k_t} \frac{1}{\hat{\delta}^2} \tag{62}$$

(iii) Third, the time needed for 90% conversion should not exceed a time T, which is dictated by technical limitations such as working hours. Equation 46 shows this to be the case if

$$K = \frac{k_d}{k_c} \ge \frac{(2 \ln(10))^3 k_t}{9 k_p{}^3 [I]_0 T^2} \tag{63}$$

These conditions imply the existence of the quasi-equilibrium regime on which they are based. This is not surprising a posteriori. Thus, taking the cube of (61), using (62) to replace one k_d, and taking the square root of the remaining expression yield

$$K = \frac{k_d}{k_c} \le \frac{\hat{\delta}\hat{\phi}^3}{\sqrt{8\pi(\ln(10))^3}} \frac{k_c [I]_0}{k_t} \tag{64}$$

In eq 64, the numerical factor in the denominator is about 17.5. Both $\hat{\delta}$ and $\hat{\phi}$ are small compared to one, and hence, (64) is just condition 26. However, the existence of the quasi-equilibrium alone does not guaranty a living and controlled radical polymerization because (61) and (62) both involve the propagation rate constant; i.e., (26) is a necessary but not a sufficient condition.

It is convenient to represent the domain of validity of the conditions 26, 61, 62, and 63 in a $k_c - k_d$ plane with logarithmic scaling. Here, conditions 61 and 63 are lines with slope 1, condition 62 is a line with slope -1, and condition 26 is a line with slope 2. These lines separate the plane into parts where the conditions are fulfilled (+ sign) and where they are not (− sign). The region where all conditions are fulfilled contains only + signs. Figure 9a displays a graph for $k_t = 10^8$ M^{-1}

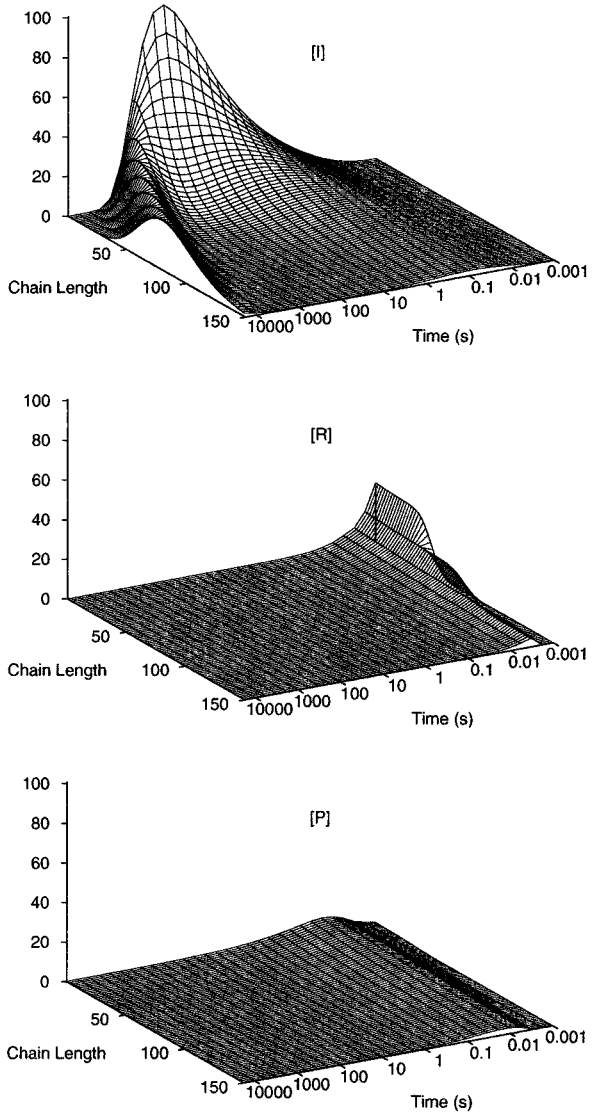

Figure 8. Chain length distributions of dormant polymer, growing radicals, and dead polymer as functions of time for $k_t = 10^8$ M^{-1} s^{-1}, $k_p = 5000$ M^{-1} s^{-1}, $k_c = 2.2 \times 10^7$ M^{-1} s^{-1}, $k_d = 4.5 \times 10^{-3}$ s^{-1}, $[I]_0 = 0.1$ M, and $[M]_0 = 10$ M.

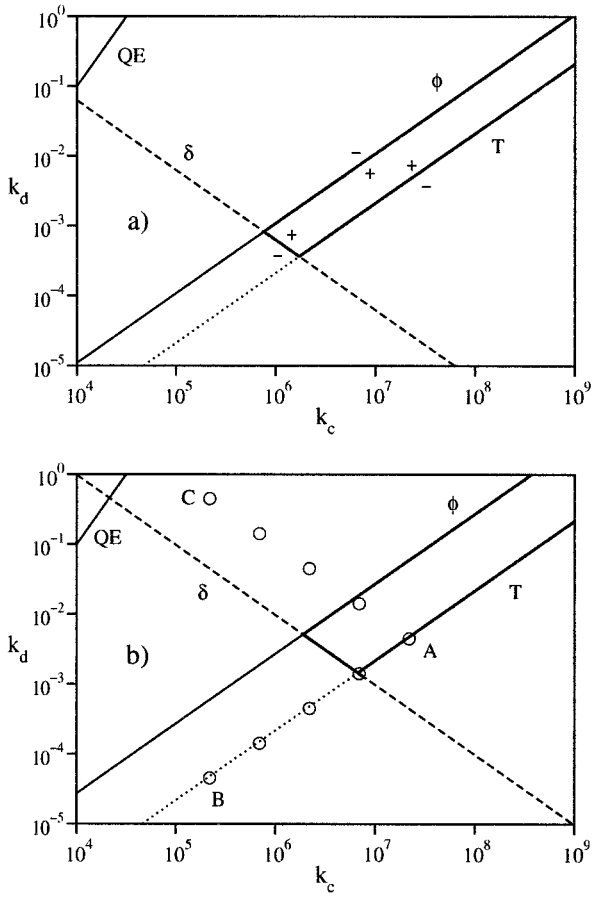

Figure 9. Graphical representations of the kinetic conditions for the existence of the quasi-equilibrium (QE), a small fraction $\phi < 5\%$ of unreactive polymer, a small residual polydispersity $\delta < 0.2$ and a time T for 90% conversion. The + sign indicates the half-plane where the condition is fulfilled, and the region where all conditions are obeyed is emphasized by a heavy frame. Key: (a) $T < 80\,000$ s (22.2 h), $k_t = 10^8$ M^{-1} s^{-1}, $k_p = 2000$ M^{-1} s^{-1}, and $[I]_0 = 0.1$ M; (b) $T < 20\,000$ s (5.55 h), $k_t = 10^8$ M^{-1} s^{-1}, $k_p = 5000$ M^{-1} s^{-1}, and $[I]_0 = 0.1$ M. The parameters (k_c,k_d) for numerical calculations are indicated by circles.

s^{-1}, $k_p = 2000$ M^{-1} s^{-1}, $[I]_0 = 0.1$ M, $\hat{\phi} = 0.05$, $\hat{\delta} = 0.2$, $T = 80\,000$ s (about 22 h). Figure 9b refers to the same parameters with the exception of a larger $k_p = 5000$ M^{-1} s^{-1} and a smaller polymerization time $T = 20\,000$ s (about 5 h). The condition for the quasi-equilibrium 26 is fulfilled nearly in the whole plane. On the other hand, the regions where the conditions for living and controlled radical polymerizations are obeyed are quite narrow. This shows again that (26) is necessary but not sufficient for successful polymerizations. In Figure 9a the optimum range of k_c extends from about $k_c = 10^6$ M^{-1} s^{-1} to the diffusion-controlled limit of $k_c = 10^9$ M^{-1} s^{-1}, and, with increasing k_c, k_d must increase from about $k_d = 10^{-3}$ to 1 s^{-1}. The line governed by $\hat{\phi}$ moves to the upper left when $[I]_0$, k_p, and $\hat{\phi}$ increase, that governed by T moves to the lower right upon increase of $[I]_0$, k_p, and T, and the line governed by $\hat{\delta}$ moves to the upper right if $[I]_0$ and k_p are increased and $\hat{\delta}$ is decreased.

The propagation and self-termination rate constants used for Figure 9a approximate the polymerization of styrene at about 120 °C. For this process and several nitroxide radicals, reasonably reliable rate constants k_d and k_c are known. These allow a gross check of our conclusions. The often used nitroxide TEMPO (2,2,6,6-tetramethylpiperidine-1-oxyl) dissociates from a polystyryl chain with a rate constant $k_d = 10^{-3}$ s^{-1}.[18] This is similar to $k_d = 5 \times 10^{-4}$ s^{-1} for the bond cleavage between TEMPO and a 1-phenylethyl group, the low molecular analogue of polystyryl.[16,17] $k_c = 7.6 \times 10^7$ M^{-1} s^{-1} for the polymeric system[18] is also similar to $k_c = 2.5 \times 10^8$ M^{-1} s^{-1} for phenylethyl.[15] These rate constants do not fall into the optimum region of Figure 9a. Hence, one would not expect a well-controlled living polymerization of styrene in relatively short times, and the insertion of the parameters into eq 63 gives a minimum time of 152 h. In practice, shorter times are achieved but it is well-known that in this case the polymerization rate is independent of the initiator concentration and is governed by the autopolymerization.[5] Other systems involve the reversible dissociation of polystyryl or phenylethyl radicals and the nitroxides SG1 (*N*-*tert*-butyl-*N*-(1-diethylphosphono-2,2-dimethylpropyl)nitroxide, $k_d = 3 \times 10^{-3}$ to 1×10^{-2} s^{-1} for polystyryl,[15,18] $k_d = 5 \times 10^{-3}$ s^{-1}, $k_c = 6 \times 10^6$ M^{-1} s^{-1} for phenylethyl,[15,17] TIPNO (*N*-*tert*-butyl-*N*-1-phenyl-2-methylpropylnitroxide, $k_d = 3.3 \times 10^{-3}$ s^{-1}, $k_c = 8 \times 10^6$ M^{-1} s^{-1} for phenylethyl[15,17]), and DBNO (di-*tert*-butylnitroxide, $k_d = 4 \times 10^{-2}$ s^{-1} for polystyryl,[18] $k_d = 1.5 \times 10^{-2}$ s^{-1}, $k_c =$

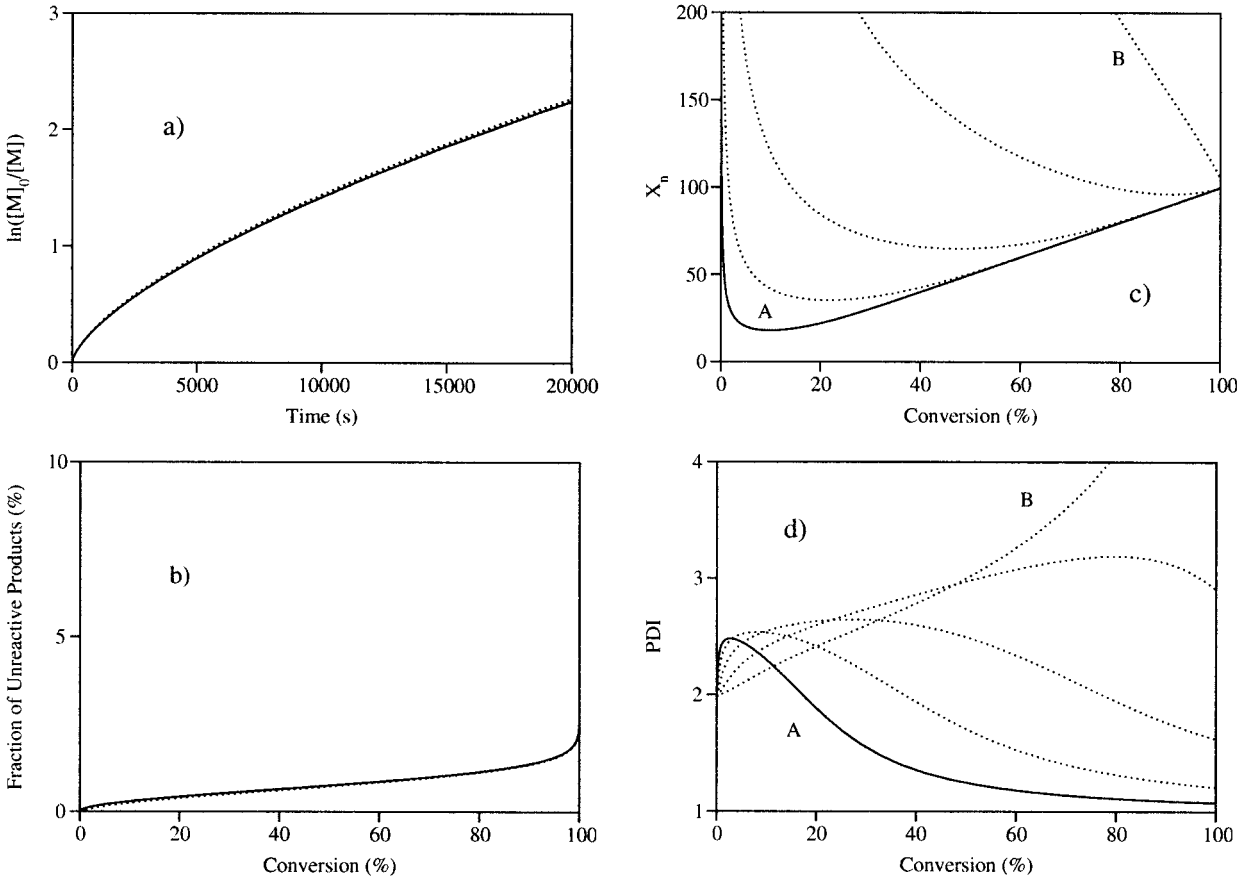

Figure 10. (a) Polymerization index $\ln([M]_0/[M])$ vs time, (b) fraction of unreactive products, (c) number-average degree of polymerization, and (d) PDI vs monomer conversion for k_c and k_d varying along line A−B in Figure 9b.

4×10^8 M^{-1} s^{-1} for phenylethyl[15b,17]). For all these systems, living radical polymerizations in reasonable times (5−8 h) have been reported which are not affected by the autopolymerization. In fact, the rate constants fall into or are very close to the optimum region of Figure 9a.

As seen in Figure 9 the condition for the existence of the quasi-equilibrium stage (QE) is fulfilled for a large range of parameters k_d and k_c and also in regions where the conditions for living and controlled polymerizations do not hold. Since there must be some effect of the quasi-equilibrium also for these cases we have performed numerical calculations for the points indicated in Figure 9b.

Point A corresponds to the parameters used already for Figures 5−8 and gives a very satisfactory living and controlled polymer. Along the line AB, k_d and k_c both decrease but the ratio $k_d/k_c = K$ remains constant. Since K determines the conversion time and the fraction of dead products these are expected to remain approximately constant. In fact, the first two parts of Figure 10 confirm this. The constant conversion time and fraction of unreactive polymer is easily understood. Along line AB, K is constant, and all points are far from a region where the quasi-equilibrium may brake down. Consequently, eq 20 gives the same concentration of transient radicals $R^\bullet$ for all points, and this causes the equal rates. Likewise, the concentrations of $Y^\bullet$ and, by stoichiometry, of P are not affected by individual changes of k_d and k_c if K remains the same. On the other hand, the other parts of Figure 10 show that the number-average degree of polymerization and the polydispersity index change drastically along line AB. This is also easily rationalized: As k_d decreases, the period of initiation increases, and hence, new chains are formed also during the conversion of monomer. The length of early born chains grows to the expected large values but short chains keep being born later on; i.e., the polydispersity must increase. The fraction of the initiator which has decomposed increases with increasing time and conversion, and this explains the decrease of X_n. For the extreme point B one obtains a polymer which is dominantly living, i.e., capped by the persistent radical. However, it has a wide chain length distribution and an average degree of polymerization which does not increase with conversion. Therefore, it is living but is not well controlled.

On line AC, the product $k_d k_c$ is constant, and, therefore, one expects an approximately constant polydispersity. Since k_d increases along the line, one also expects that the number-average degree of polymerization X_n behaves close to the ideal case. On the other hand, the polymerization becomes faster, and the points deviate increasingly from the condition for a low fraction of dead polymer. The results of the numerical calculations (Figure 11) confirm these expectations: Apart from point C for which the condition for the quasi-equilibrium is breaking down, X_n and PDI are very similar as in the ideal case A. The polymerization time shortens (except for C), and for large conversions there are large fractions of unreactive polymer. Thus, under these conditions one obtains polymers which are controlled from the view of the molecular weight distribution but they are not fully living in the sense of extendable chains.

Effects of Varying Rate Constants. In polymerizing systems the rate constants k_d, k_c, k_p, and k_t of the

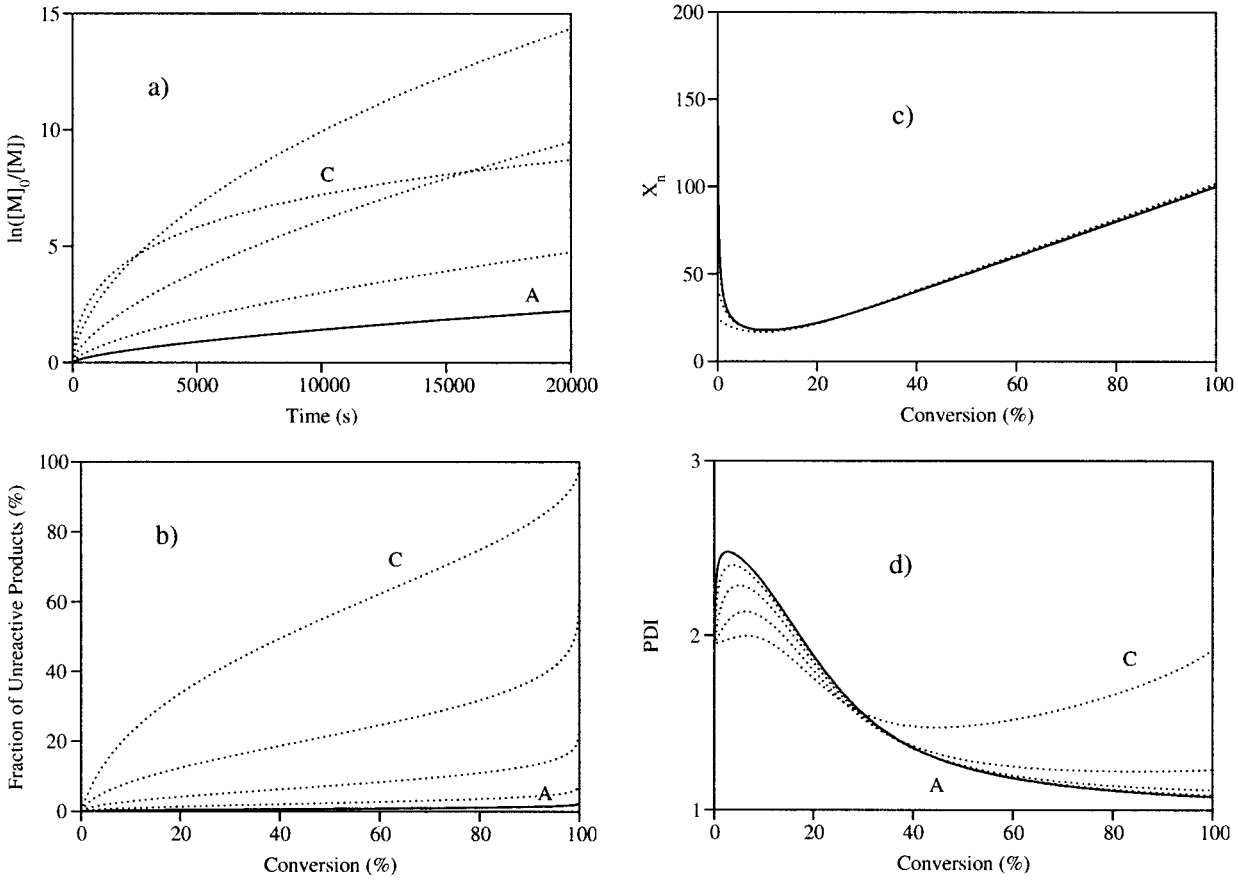

Figure 11. (a) Polymerization index $\ln([M]_0/[M])$ vs time, (b) fraction of unreactive products, (c) number-average degree of polymerization, and (d) PDI vs monomer conversion for k_c and k_d varying along line A−C in Figure 9b.

basic reactions (eqs 1−4) are expected to depend on the chain length n of the dormant polymers R_n−Y and of the propagating radicals $R_n^\bullet$. Moreover, the rate constants for the bimolecular reactions k_c, k_p, and k_t are also expected to depend on the diffusion coefficients of the reaction partners and, hence, on the viscosity, which increases with monomer conversion. Therefore, a discussion of the deviations from our theoretical predictions which may be caused by varying rate constants is in place.

A recent systematic study of the factors influencing the bond dissociation rates of alkoxyamines[17] has reveiled that there are only moderate rate enhancing influences of a large steric demand of the alkyl groups which do not exceed a factor of 10. Also, the comparison of experimental rate constants k_d for the dissociation of alkoxyamines with long polymer chains and with their low molecular weight analogues does not reveal large differences (120 °C: polystyryl−TEMPO,[18] $k_d = 10^{-3}$ s^{-1}, vs phenylethyl−TEMPO,[16,17] $k_d = 5 \times 10^{-4}$ s^{-1}; polystyryl−SG1,[15] $k_d = 3 \times 10^{-3}$ to 1×10^{-2} s^{-1}, vs phenethyl−SG1,[17] $k_d = 5 \times 10^{-3}$ s^{-1}; and poly-*n*-butylacylate−SG1,[15] $k_d = 7 \times 10^{-3}$ s^{-1}, vs 1-methoxycarbonylethyl,[17] $k_d = 3 \times 10^{-3}$ s^{-1}) though there is a tendency for larger rate constants at larger chain length. Overall, however, the effect is small and should not give large deviations from the theoretical results.

The rate constants k_c for the coupling of alkyl with nitroxide radicals depend strongly on the nitroxide and alkyl structures and to a smaller extent on solvent and viscosity, and one may expect a decrease with increasing chain length and viscosity.[14,15] There are only very few data for comparison such as for polystyryl + TEMPO, $k_c = 7.6 \times 10^7$ M^{-1} s^{-1} vs $k_c = 2.5 \times 10^8$ M^{-1} s^{-1} for phenylethyl + TEMPO at 125 °C,[15,18] and polystyryl + SG1, $k_c = 7 \times 10^5$ M^{-1} s^{-1} vs phenethyl + SG1, 5×10^6 M^{-1} s^{-1} at 120 °C.[15,18] For *n*-butylacrylyl + SG1 one has $k_c = 4 \times 10^7$ M^{-1} s^{-1} at 120 °C, [15] and the value for a low molecular analogue should be intermediate between 8×10^8 M^{-1} s^{-1} for methoxycarbonylmethyl and 2×10^6 M^{-1} s^{-1} for 2-methoxycarbonyl-2-propyl.[15] Obviously, the effect of chain length on k_c is also not drastic.

Propagation rate constants k_p are generally believed to decrease with increasing chain length but, for low conversion, only for the few first addition steps.[22] A recent comparison of addition rate constants of structurally similar small alkyl radicals with their polymeric counterparts[23] revealed a decrease by a factor of about 10 which is due to the larger steric demand of the latter radicals. This limited effect should also not affect the overall validity of our conclusions for real systems. However, at extreme conversions (> 85%), k_p is known to decrease strongly, so the treatment is only valid for limited conversions.

More serious is the decrease of the self-termination rate constant k_t with increasing chain length and viscosity. On the basis of simulations, Matyjaszewski et al.[24] recently claimed that this may severely mask the persistent radical effect insofar as $\ln[M]_0/[M]$ does not show the $t^{2/3}$ dependence of eq 44. Actually, this equation itself suggests a weaker dependence if k_t decreases in time, and experimentally one often finds a more linear dependence conforming to eq 45. For conventional radical polymerizations the drastic reductions of k_t with increasing chain length and conversion leads to an autoacceleration of the polymerization which

is also called the Trommsdorff−Norrish or gel effect.[2] Many theoretical models for this effect have been advanced[25] but they all consider the conventional case where fairly long chains ($X_n > 100$) are present throughout the polymerization. In the living process there are (a few, see above) long chain radicals formed at the beginning, but then the chains grow continuously to the final length, and one seldom aims at very large molecular weights. Hence, except for very high conversions the effects of restriced diffusion, e.g. by chain entanglement, should be less expressed. In fact, this was stated by Georges et al.[26] who did not find a large gel effect for the living radical polymerization of styrene in bulk up to a molecular weight of 80 000 and up to 80% conversion. Nevertheless, the probable reduction of k_t requires a closer exploration of its effects. Therefore, we repeated the simulations of Matyjaszewski et al.[24] with some modifications and extensions. These authors started from the diffusion coefficients D of methyl methacrylate and butyl methacrylate oligomers ($n = 1-10$) measured by Gilbert et al.[27] in polymer matrices of methyl methacrylate and butyl methacrylate at 25 and 40 °C which were swollen with methyl isobutyrate and butyl isobutyrate to various degrees. The results obeyed the universal equation

$$\frac{D(n)}{D(1)} = n^{-(0.664 + 2.02w_p)} \tag{65}$$

where w_p is the mass fraction of the polymer matrix. The polymers had number-average molecular weights of 1×10^5 and 1.5×10^5, respectively, and large polydispersities of 2.5 and 1.9. The mass fraction w_p was varied from 0.1 to 0.5, and eq 65 was found to hold for styrene oligomers in polystyrene matrices as well. For the simulation, Matyjaszewski et al.[24] set $k_t(n)$ proportional to $D(n)$ and approximated the chain length n by the number-average degree of polymerization X_n. This, in turn, was set proportional to the monomer conversion C as $X_n = ([M]_0 - [M])/[I]_0 = (([M]_0 - [M])/[M]_0)[M]_0/[I]_0 = C[M]_0/[I]_0$ under neglect of the effect of residual initiator (eq 57). The weight fraction of polymer is equal to the conversion. With a ratio of initial monomer to initiator concentration of 100, this casts eq 65 into a conversion dependent form

$$k_t(C(t)) = k_t(0)(100C(t))^{-(0.65+2.0C(t))} \tag{66}$$

which was more easily accommodated by the simulation routine than the original equation. A reasonable $k_t(0) = 10^9$ M^{-1} s^{-1} was adopted.

In the following, we adhere more strictly to eq 65 and treat the chain-length and conversion dependence explicitly as

$$k_t(n) = k_t(0)n^{-(\alpha+\beta C(t))}. \tag{67}$$

The termination constant at low viscosity and chain length $k_t(0) = 10^9$ M^{-1} s^{-1} is adopted, and for the cross-termination constants of radicals with different length we use the geometric mean

$$k_t(m,n) = (k_t(m)k_t(n))^{1/2} \tag{68}$$

Similarly as for Figure 8, the individual coupled kinetic equations for I_n, $R_n^\bullet$, P_n, $Y^\bullet$, and M were integrated with $n = 0$ to 160 and $n > 160$ as closure terms and for the parameters $[M]_0 = 10$ M, $[I]_0 = 0.1$ M, i.e., $[M]_0/[I]_0 = 100$, $k_p = 2000$ M^{-1} s^{-1}, $k_c = 5 \times 10^6$ M^{-1} s^{-1}, and $k_d = 5 \times 10^{-3}$ s^{-1}. The parameters of eq 67 were varied as $\alpha = 0$, 0.2, 0.4, 0.6, and 0.8 and $\beta = 0$, 0.5, 1.0, 1.5, and 2.0, and the average of k_t was calculated for each time from eq 69.

$$k_t = \frac{\sum_{m,n} k_t(m,n)[R_m][R_n]}{\sum_{m,n}[R_m][R_n]} \tag{69}$$

Matyjaszewski et al.[24] used $\alpha = 0.65$ and $\beta = 2.0$. In view of the lower chain length dependence of $k_t \propto n^{-0.2}$ established from pulse laser photolysis polymerizations at low conversions and in view of probably weaker conversion dependence for living systems, especially at higher temperatures, these parameters are probably upper extremes.

Figure 12 shows the results for the relatively large $\alpha = 0.6$ and the different values of β. In general, α has a rather small effect. For $\beta = 0$, the average termination constant (Figure 12a) drops initially from $k_t = 10^9$ M^{-1} s^{-1} to about $k_t = 10^8$ M^{-1} s^{-1} because of the formation of radicals with extended chains at the beginning of the process (Figure 8). Then it increases again as the fraction of these radicals diminishes, and finally there is a smooth decrease to the final $k_t = 10^8$ M^{-1} s^{-1}. Hence, the chain length dependence of k_t alone does not produce drastic changes of the course of the polymerization. However, with increasing β, k_t drops strongly with increasing conversion and reaches the low values calculated by Matyjazsewski et al.[24] Figure 12b shows the corresponding developments of the radical and the monomer concentrations. Obviously, the decrease of k_t does not affect the initial period with the establishment of unequal concentrations of R$^\bullet$ and Y$^\bullet$ which is characteristic for the persistent radical effect. Later on, it causes a weakening of the radical time dependencies, and in particular of the decrease of [R]. This, in turn, increases the monomer conversion rate, and a comparison of Figure 5 with Figure 12c demonstrates that ln $([M]_0/[M])$ grows indeed more linearly in time if the conversion dependence of k_t is taken into account. Interestingly, the decrease of k_t has practically no effect on the average degree of polymerization and on the polydispersity (Figure 12, parts d and e), and Figure 12f shows that it has a small favorable effect on the fraction of unreactive products. Moreover, linear fits of conversion curves (Figure 12c) for different initiator concentrations showed apparent reaction orders which were only weakly dependent on β and decreased with increasing α from 0.33 as for constant termination constants (Figure 5) to 0.15. These results show that the chain-length and conversion dependence of the termination constant can affect the polymerization kinetics in detail but do not alter the principal features for its control by the persistent radical effect.

Concluding Remarks

As in the previous theoretical work[9] we have concentrated on the analytical description of living free radical polymerizations based on reversible bond cleavage and the minimal set of required reactions (eqs 1−4). Numerical simulations were used to check the validity of the analytic equations, for illustrations and cases where

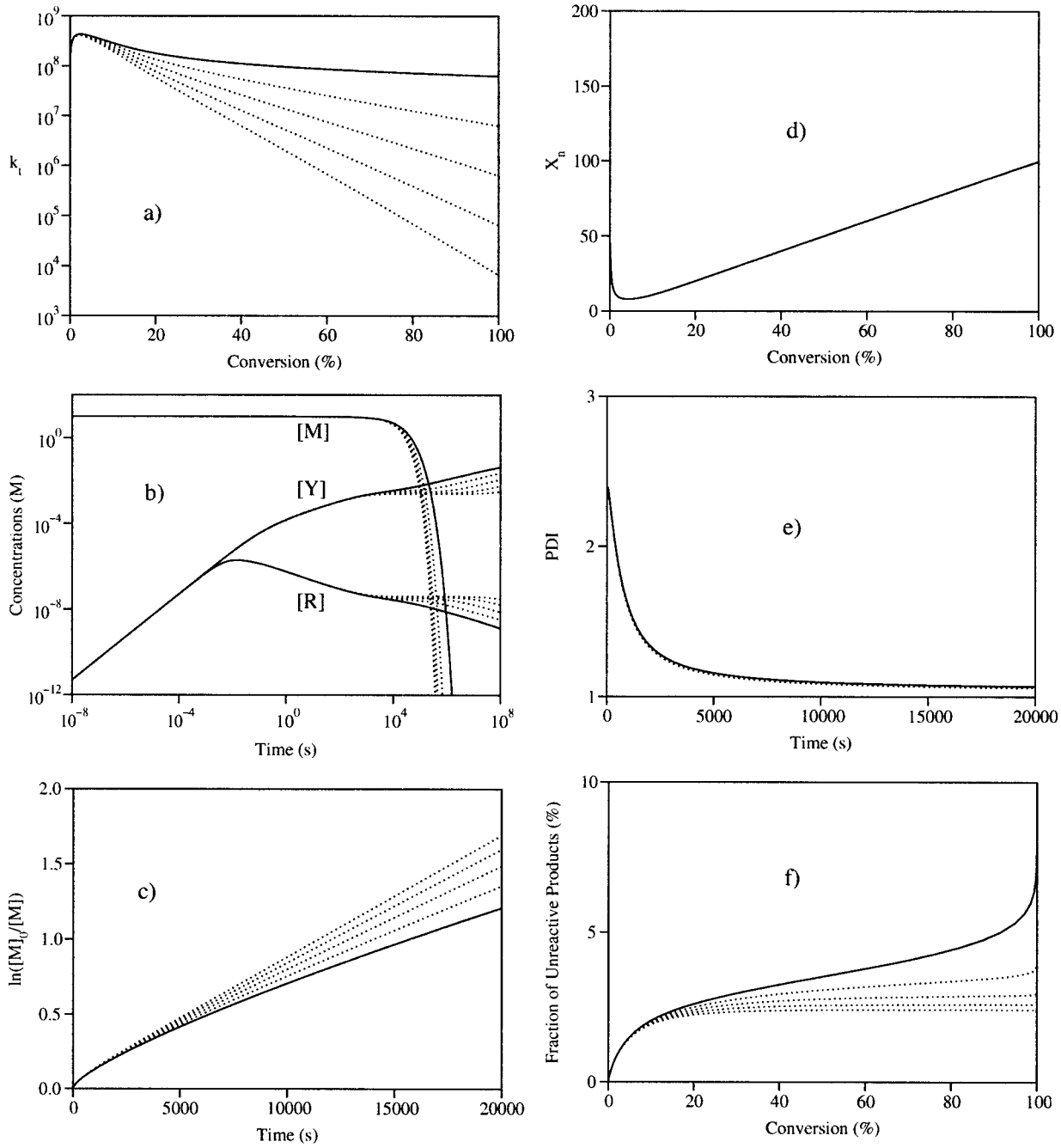

Figure 12. Effects of chain-length and conversion dependent termination constants. $\alpha = 0.6$ and $\beta = 0$, 0.5, 1.0, 1.5, and 2.0, respectively. Key: (a) k_t vs conversion; (b) concentrations of radicals and monomer vs time; (c) $\ln([M]_0/[M])$ vs time; (d) number-average degree of polymerization vs conversion; (e) PDI vs time; (f) fraction of unreactive products vs conversion. For other parameters, see text.

the equations break down. An earlier analytic modeling neglected the self-termination (eq 4) of the transient radicals completely.[28] This oversimplification leads to simpler mathematics but also to equal concentrations of transient and persistent radicals which are in contrast to observation. Consequently, the neglect of self-termination does not even approximate realistic systems. Several purely numeric solutions of the kinetic equations with chain-length independent rate constants are also available. A comparison with our results reveals that they offer only partial views of the process because they were carried out for limited ranges of the relevant rate constants. Thus, Johnson et al.[29] correctly stated that the mechanism cannot lead to stationary radical concentrations and also gave the correct reason for the permanently increasing excess of the persistent over the transient radicals. Large dissociation rate constants k_d gave fast polymerizations, and therefore, alkoxyamines were recommended, which decay as fast as practical. This misses the fact that too large rate constants lead to a breakdown of the persistent radical effect. He et al.[30] calculated the correct nonlinear dependence of the conversion rate on time and its scaling with the equilibrium constant of the dissociation and not with k_d alone. However, they misinterpreted the low transient radical concentration as a stationary state. Finally, Zhu[31] noticed the correct influence of the propagation and cross-termination rate constants k_p and k_c on the polydispersity but their inclusion of unnecessary side reactions complicated the pattern. For rate constants

fulfilling the conditions given above, such numerical work can now be replaced by simpler plotting procedures based on analytical equations.

Finally, we wish to comment on the typical characteristics of living free radical polymerizations mediated by reversible dond dissociation because some of the often cited analogies with ionic living processes are not straightforward.

In ideal ionic living polymerizations, the concentration of the growing chains matches that of the counterions; i.e., there are true equilibria, whereas in living radical polymerizations there is a quasi-equilibrium with a large excess of the persistent over the transient species. Both mechanisms produce polymers with reactive end groups. However, in ideal ionic polymerizations self-termination reactions are truely absent whereas in the radical mechanism some fraction of unreactive polymers is always formed. The self-termination is even essential for the establishment of the quasi-equilibrium and the polymerization control, and it occurs not only at the onset but also during the whole process. Therefore, it is not an unwanted (and eventually avoidable) side reaction, and a living radical polymerization is not really a polymerization without termination. Yet, the termination products may be very minor fractions, indeed.

As in ionic processes, a linear increase of the average degree of polymerization and a decrease of the polydispersity with conversion are clear evidence for the living process, and deviations such as presented in Figures 7, 10, and 11 may be indicative for the radical pathway. However, and in contrast to ionic processes a constant rate of propagation and a linear dependence of $\ln([M]_0/[M])$ on time does not characterize a living radical polymerization. For chain-length independent rate constants a weaker time dependence should hold (Figure 5) although this may be blurred by the chain-length dependence of the self-termination constant (vide supra). Further, there are often side effects which provide steady state radical concentrations such as an voluntary or unvoluntary initial excess of the persistent species, extra self-initiations or other initiations or an irreversible decay of the persistent species to transient radicals. The formulation of the theory for these cases is underway. In any case, for a living radical polymerization, the apparent reaction order with respect to the initiator concentration should be significantly lower than that for ionic mechanisms.[1,2]

Acknowledgment. We thank the Swiss National Foundation for Scientific Research for financial support, Prof. D. Evans, Canberra, for pointing out the use of phase diagram analyses, and S. Schafroth for help in the early stages of the numerical parts of this work.

Appendix. Kinetic Conditions for the Quasi-Equilibrium

We seek necessary and sufficient conditions for the parameters a and b (eq 15) such that there exists a part of the trajectory in the (ρ,η)-phase plane where the quasi-equilibrium relation 21 is obeyed, i.e., where one has

$$1 - \epsilon < a\rho\eta < 1 \tag{A1}$$

with arbitrarily small ϵ. From the phase diagram analysis this part of the trajectory is located above the isocline $\dot{\rho} = 0$ and below $\dot{\eta} = 0$. Hence, eqs 24 and 25 for the isoclines give the condition

$$1 - b\rho^2 - \eta < a\rho\eta < 1 - \eta \tag{A2a}$$

One also has for the whole trajectory

$$\rho \le \eta \tag{A2b}$$

and

$$\rho \le \frac{1}{\sqrt{b}} \tag{A2c}$$

Necessary Conditions. (1) From (A1) and (A2a), it is necessary that $\eta < \epsilon$. Then from (A1)

$$a\rho > \frac{1-\epsilon}{\eta} > \frac{1-\epsilon}{\epsilon} \tag{A3}$$

Combination with (A2c) gives

$$\frac{1-\epsilon}{a\epsilon} < \rho \le \frac{1}{\sqrt{b}} \tag{A4}$$

which implies

$$\frac{a^2}{b} > \left(\frac{1-\epsilon}{\epsilon}\right)^2 \tag{A5}$$

For $\epsilon \ll 1$, (A5) reads

$$\frac{a^2}{b} \gg 1 \tag{A6}$$

which is condition 26 of the main text.

(2) From (A1) and (A2b) one has $a\eta^2 \ge a\rho\eta > 1 - \epsilon$, which implies that

$$a > \frac{1-\epsilon}{\eta^2} > \frac{1-\epsilon}{\epsilon^2} \tag{A7}$$

Hence, for $\epsilon \ll 1$ we must have

$$a \gg 1 \tag{A8}$$

which is condition 27 of the main text.

Sufficient Conditions. (1) To obtain (A1) from (A2a), it is sufficient to have

$$\eta < \frac{\epsilon}{2} \quad \text{and} \quad b\rho^2 < \frac{\epsilon}{2} \tag{A9}$$

Rearrangement of (A2a) and squaring provides

$$b\rho^2 < b\,\frac{(1-\eta)^2}{a^2\eta^2} \tag{A10}$$

Therefore, it is sufficient to have

$$\eta < \frac{\epsilon}{2} \quad \text{and} \quad b\frac{(1-\eta)^2}{a^2\eta^2} < \frac{\epsilon}{2} \tag{A11}$$

These conditions are fulfilled if η is in the interval $\eta_l < \eta < \eta_u$ with

$$\eta_l = \frac{1}{1 + \frac{a}{\sqrt{b}}\sqrt{\frac{\epsilon}{2}}} \quad \text{and} \quad \eta_u = \frac{\epsilon}{2} \tag{A12}$$

and this interval exists if a and b fulfill

$$\frac{1}{1 + \frac{a}{\sqrt{b}}\sqrt{\frac{\epsilon}{2}}} < \frac{\epsilon}{2} \tag{A13}$$

which implies

$$\frac{a^2}{b} > \frac{\left(1 - \frac{\epsilon}{2}\right)^2}{\left(\frac{\epsilon}{2}\right)^3} \tag{A14}$$

(A13) is also valid if a and b fulfill

$$\frac{1}{1 + \frac{a}{\sqrt{b}}\sqrt{\frac{\epsilon}{2}}} < \frac{\epsilon}{4} \tag{A15}$$

which rearranges to

$$\frac{a^2}{b} > \frac{1\left(1 - \frac{\epsilon}{4}\right)^2}{2\left(\frac{\epsilon}{4}\right)^3} \tag{A16}$$

For $\epsilon \ll 1$, both (A14) and (A16) give

$$\frac{a^2}{b} \gg 1 \tag{A6}$$

which is condition 26 of the main text.

(2) If η is in the interval $\eta_i < \eta < \eta_u$ with $\eta_i = \epsilon/4$, (A2a) provides

$$\rho < \frac{1 - \eta}{a\eta} < \frac{1 - \eta_i}{a\eta_i} \tag{A17}$$

To ensure that (A2b) is also valid in this interval, it suffices to have

$$\frac{1 - \eta_i}{a\eta_i} < \eta_i \tag{A18}$$

that is

$$a > \frac{1 - \frac{\epsilon}{4}}{\left(\frac{\epsilon}{4}\right)^2} \tag{A19}$$

which gives for $\epsilon \ll 1$

$$a \gg 1 \tag{A8}$$

i.e., again condition 27 of the main text. Hence, conditions A6 and A8 are necessary and sufficient for the existence of the quasi-equilibrium.

It should be noted that (A6) follows as a sufficient condition already from the wider interval (A13) but the derivation of (A8) requires the stronger limitation (A15). In essence, condition A16 guaranties the existence of a region R of the phase plane between the two isoclines $\dot{\rho} = 0$ and $\dot{\eta} = 0$, with $\epsilon/4 < \eta < \epsilon/2$, where all points (ρ,η) satisfy (A1). Condition A19 ensures in addition that R is located above the diagonal $\eta = \rho$. The trajectory passes necessarily through R because, after crossing $\dot{\rho} = 0$, it is confined to the space between the isoclines and because it obeys $\eta \geq \rho$.

References and Notes

(1) Szwarc, M. *J. Polym. Sci.* **1998**, *A36*, ix.

(2) Young, R. J.; Lovell, P. A. *Introduction to Polymers*, 2nd ed.; Chapman & Hall: London, 1991. Elias, H.-G. *Macromolecules*, 2nd ed.; Plenum: New York, 1984.

(3) Solomon, D. H.; Rizzardo, E.; Cacioli, P. U.S. Pat. 4 581 429; *Chem. Abstr.* **1985**, *102*, 221335q.

(4) Georges, M. K.; Veregin, R. P. N.; Kazmaier, P. M.; Hamer, G. K. *Macromolecules* **1993**, *26*, 2987.

(5) Kazmaier, P. M.; Moffat, K. A.; Georges, M. K.; Veregin, R. P. N.; Hamer, G. K. *Macromolecules* **1995**, *28*, 1841. Georges, M. K.; Hamer, G. K.; Listigovers, N. A. *Macromolecules* **1998**, *31*, 9087. Bon, S. A. F.; Bosveld, M.; Klumperman, B.; German, A. L. *Macromolecules* **1997**, *30*, 324. Fukuda, T.; Goto, A.; Ohno, K.; Tsujii, Y. *ACS Symp. Ser.* **1998**, *685*, 180. Ohno, K.; Izu, Y.; Yamamoto, S.; Miyamoto, T.; Fukuda, T. *Macromol. Chem. Phys.* **1999**, *200*, 1619. Jousset, S.; Hammouch, S. O.; Catala, J.-M. *Macromolecules* **1997**, *30*, 6685. Benoit, D.; Grimaldi, S.; Finet, J. P.; Tordo, P.; Fontanille, M.; Gnanou, Y. *ACS Symp. Ser.* **1998**, *685*, 225. Benoit, D.; Chaplinski, V.; Braslau, R. J.; Hawker, C. J. *J. Am. Chem. Soc.* **1999**, *121*, 3904. Li, I. Q.; Howell, B. A.; Dineen, M. T.; Kastl, P. E.; Lyons, J. W.; Meunier, D. M.; Smith, P. B.; Priddy, D. B. *Macromolecules* **1997**, *30*, 5195. Puts, R. D.; Sogah, Y. *Macromolecules* **1996**, *29*, 3323. Lokaj, J.; Vlcek, P.; Kriz, J. *Macromolecules* **1997**, *30*, 7644. Yoshida, E.; Okada, Y. *Macromolecules* **1998**, *31*, 1446. Leduc, M. R.; Hawker, C. J.; Dao, J.; Frechet, J. M. J. *J. Am. Chem. Soc.* **1996**, *118*, 11111. Steenbock, M.; Klapper, M.; Muellen, K.; Bauer, C.; Hubrich, M. *Macromolecules* **1998**, *31*, 5223. Hoelderle, M.; Baumert, M.; Muelhaupt, R. *Macromolecules* **1997**, *30*, 3420. Druliner, J. D. *J. Phys. Org. Chem.* **1995**, *8*, 316. Wayland, B. B.; Basickes, L.; Mukerjee, S.; Wei, M.; Fryd, M. *Macromolecules* **1997**, *30*, 8109. Wayland, B. B.; Poszmik, G.; Mukerjee, S. L. *J. Am. Chem. Soc.* **1994**, *116*, 7943. Chung, T. C.; Janvikul, W.; Lu, H. L. *J. Am. Chem. Soc.* **1996**, *118*, 705. Chong, Y. K.; Ercole, F.; Moad, G.; Rizzardo, E.; Thang, S. H.; Anderson, A. G. *Macromolecules* **1999**, *32*, 6895. Han, C. H.; Drache, M.; Baethge, H.; Schmidt-Naake, G. *Macromol. Chem. Phys.* **1999**, *200*, 1779. Yoshida, E.; Tanimoto, S. *Macromolecules* **1997**, *30*, 4018. Bergbreiter, D. E.; Walchuk, B. *Macromolecules* **1998**, *31*, 6380 and references therein.

(6) Otsu, T.; Yoshida, M.; Tazaki, T. *Macromol. Rapid Commun* **1982**, *3*, 133.

(7) Otsu, T.; Tazaki, T.; Yoshioka, M. *Chem. Express* **1990**, *5*, 801. Kato, M.; Kamigaito, M.; Sawamoto, M.; Higashimura, T. *Macromolecules* **1995**, *28*, 1721. Wang, J. S.; Matyjaszewski, K. *J. Am. Chem. Soc.* **1995**, *117*, 5614; *Macromolecules* **1995**, *28*, 7901. Percec, V.; Barboiu, B. *Macromolecules* **1995**, *28*, 7970. Matyjaszewski, K. *Macromolecules* **1998**, *31*, 4710; *J. Macromol. Sci.—Pure. Appl. Chem.* **1997**, *A 34*, 1785. Haddleton, D. M.; Jasieczek, C. B.; Hannon, M. J.; Shooter, A. J. *Macromolecules* **1997**, *30*, 2190. Jankova, K.; Chen, X.; Kops, J.; Batsberg, W. *Macromolecules* **1998**, *31*, 538. Percec, V.; Kim, H.-J.; Barboiu, B. *Macromolecules* **1997**, *30*, 8526. Ueda, J.; Matsuyama, M.; Kamigaito, M.; Sawamoto, M. *Macromolecules* **1998**, *31*, 557. Moineau, G.; Granel, C.; Dubois, P.; Jerome, R.; Teyssie, P. *Macromolecules* **1998**, *31*, 542.

(8) Chiefari, J.; Chong, Y. K.; Ercole, F.; Krstina, J.; Jeffery, J.; Lee, T. P. T.; Mayadunne, R. T. A.; Meijs, G. F.; Moad, C. L.; Moad, G.; Rizzardo, E.; Thang, S. H. *Macromolecules* **1998**, *31*, 5559. Hawthorne, D. G.; Moad, G.; Rizzardo, E.; Thang, S. H. *Macromolecules* **1999**, *32*, 5457.

(9) Fischer, H. *Macromolecules* **1997**, *30*, 5666; *J. Polym. Sci. A* **1999**, *37*, 1885.

(10) Perkins, M. J. *J. Chem. Soc.* **1964**, 5932. Fischer, H. *J. Am. Chem. Soc.* **1986**, *108*, 3925. Ruegge, D.; Fischer, H. *Int. J. Chem. Kinet.* **1989**, *21*, 703. Kothe, T.; Martschke, R.; Fischer, H. *J. Chem. Soc., Perkin Trans. 2* **1998**, 503. Wagner, P. J.; Thomas, M. J.; Puchalski, A. E. *J. Am. Chem. Soc.* **1986**, *108*, 7739. Walling, C. *J. Am. Chem. Soc.* **1988**, *110*, 6846. Daikh, E.; Finke, R. G. *J. Am. Chem. Soc.* **1992**, *114*, 2939. MacFaul, P. A.; Arens, I. W. C. E.; Ingold, K. U.; Wayner, D. D. M. *J. Chem Soc., Perkin Trans. 2* **1997**, 135. Bravo, A.; Bjorsvik, H.-R.; Fontana, F.; Liguori, L.; Minisci, F. *J. Org. Chem.* **1997**, *62*, 3849. Karatekin, E.; O'Shaughnessy, B.; Turro, N. J. *J. Chem. Phys.* **1998**, *108*, 9577.

(11) Since two radicals R$^\bullet$ disappear in the self-termination reaction the corresponding term in eq 13 should properly be written as $-2k_t[R]^2$. We abbreviate $2k_t$ as k_t to avoid the crowding of subsequent formulas with factors of 2.

(12) Fischer, H.; Paul, H. *Acc. Chem. Res.* **1987**, *20*, 200.

(13) Beuermann, S.; Buback, M. *ACS Symp. Ser.* **1998**, *685*, 84.

(14) Chateauneuf, J.; Lusztyk, J.; Ingold, K. U. *J. Org. Chem.* **1988**, *53*, 1629. Beckwith, A. L. J.; Bowry, V. W.; Ingold, K. U. *J. Am. Chem. Soc.* **1992**, *114*, 4983. Bowry, V. W.; Ingold, K. U. *J. Am. Chem. Soc.* **1992**, *114*, 4992. Beckwith, A. L. J.; Bowry, V. W.; Moad, G. *J. Org. Chem.* **1988**, *53*, 1632. Baldovi, M. V.; Mohtat, N.; Scaiano, J. C. *Macromolecules* **1996**, *29*, 5497.

(15) LeMercier, C.; LeMoigne, F.; Tordo, P.; Lutz, J.-F.; Lacroix-Desmazes, P.; Boutevin, B.; Couturier, J.-L.; Guerret, O.; Marque, S.; Martschke, R.; Sobek, J.; Fischer, H. *ACS Symp. Ser.* **2000**, *768*, 108. Sobek, J.; Martschke, R.; Fischer, H. To be published. Benoit, D.; Grimaldi, S.; Robin, S.; Finet, J.-P.; Tordo, P.; Gnanou, Y. *J. Am. Chem. Soc.* **2000**, *122*, 5929.

(16) Moad, G.; Rizzardo, E. *Macromolecules* **1995**, *28*, 8722. Skene, W. G.; Belt, S. T.; Connolly, T. J.; Hahn, P.; Scaiano, J. C. *Macromolecules* **1998**, *31*, 9103. Ciriano, M. V.; Korth, H. G.; van Scheppingen, W. B.; Mulder, P. *J. Am. Chem. Soc.* **1999**, *121*, 6375. Connolly, T. J.; Baldovi, M. V.; Mohtat, N.; Scaiano, J. C. *Tetrahedron Lett.* **1996**, *37*, 4919.

(17) Marque, S.; LeMercier, C.; Tordo, P.; Fischer, H. *Macromolecules* **2000**, *33*, 4403.

(18) Goto, A.; Terauchi, T.; Fukuda, T.; Miyamoto, T. *Macromol. Rapid Commun.* **1997**, *18*, 673. Goto, A.; Fukuda, T. *Macromolecules* **1999**, *32*, 618. Bon, S. A. F.; Chambard, G.; German, A. L. *Macromolecules* **1999**, *32*, 8269. Fukuda, T.; Goto, A.; Ohno, K. *Macromol. Rapid Comm.* **2000**, *21*, 151.

(19) Kothe, T.; Marque, S.; Martschke, R.; Popov, M.; Fischer, H. *J. Chem. Soc., Perkin Trans. 2* **1998**, 1553.

(20) Hubbard, J. H.; West, B. H. *Differential Equations: A Dynamical Systems Approach, Part II*; Springer: Berlin, 1995.

(21) Ohno, K.; Tsujii, Y.; Miyamozo, T.; Fukuda, T.; Goto, A.; Kobayashi, K.; Akaike, T. *Macromolecules* **1998**, *31*, 1064.

(22) Moad, G.; Solomon, D. H. *The Chemistry of Free Radical Polymerization*; Pergamon: Oxford, England, 1995. Moad, G.; Rizzardo, E.; Solomon, D. H.; Beckwith, A. L. J. *Polym. Bull.* **1992**, *29*, 647.

(23) Fischer, H.; Radom, L. *Angew. Chem.*, to be published.

(24) Shipp, D. A.; Matyjazsewski, K. *Macromolecules* **1999**, *32*, 2948.

(25) Litvinenko, G. I.; Kaminski, V. A. *Prog. React. Kinet.* **1994**, *19*, 139.

(26) Saban, M. D.; Georges, M. K.; Veregin, R. P. N.; Hamer, G. K.; Kazmaier, P. M. *Macromolecules* **1995**, *28*, 7032.

(27) Griffith, M. C.; Strauch, J.; Monteiro, M. J.; Gilbert, R. G. *Macromolecules* **1998**, *31*, 7835.

(28) Yan, D.; Jiang, H.; Fan, X. *Macromol. Theory Simul.* **1996** *5*, 333.

(29) Johnson, C. H. J.; Moad, G.; Solomon, D. H.; Stirling, T. H.; Vearing, D. J. *Austr. J. Chem.* **1990**, *43*, 1215.

(30) He, J.; Zhang, H.; Chen, J.; Yang, Y. *Macromolecules* **1997**, *30*, 8010.

(31) Zhu, S. *J. Polym. Sci., B: Polym. Phys.* **1999**, *37*, 2692.

MA000689S